



Canadian Space
Agency

Agence spatiale
canadienne



*Ten Years
of CASSIOPE:
A Canadian
Space Science
Success Story*

Andrew Howarth

DASP 2024

February 21, 2024

Edmonton, Alberta




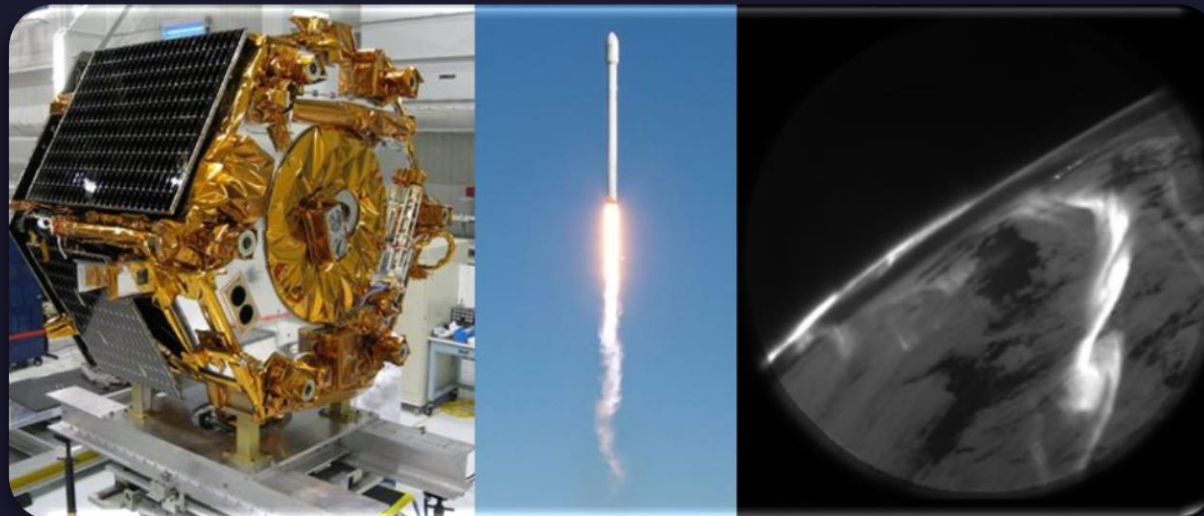
UNIVERSITY OF
CALGARY



Mission Overview



Spacecraft	 Small satellite, 125 cm x 180 cm
Names	CASSIOPE/e-POP/Swarm-Echo
Launch	September 29, 2013
Support	CSA, Government of Canada, MDA, ESA, University of Alaska Fairbanks
Orbit	325 x 1500 km, 81° inclination, non-sun-synchronous
Attitude	3-axis stabilized until 2021, then spin-stabilized (6 min period)



Science Payload



HF Beacon Transmitter

150/400/1066 MHz

CERTO

Auroral Imager

650–1000 nm; 630 nm

FAI

GPS Receivers

5 units, L1 and L2

GAP

Ion Mass Spectrometer

0.5-70 eV/q; 1-40 amu/q

IRM

Magnetometer

Dual mags, 160 samples/s

MGF

Radio Receiver

0.01-18 MHz; 31.25 kHz bandwidth

RRI

Electron Imager

0.1-350 eV ions or electrons

SEI

Highlights from the last 10 years



Radio Science – *SuperDARN*

Auroral Dynamics

M-I-T Coupling

Radio Science – *Citizen Science*

Radio Science – *HF Propagation*

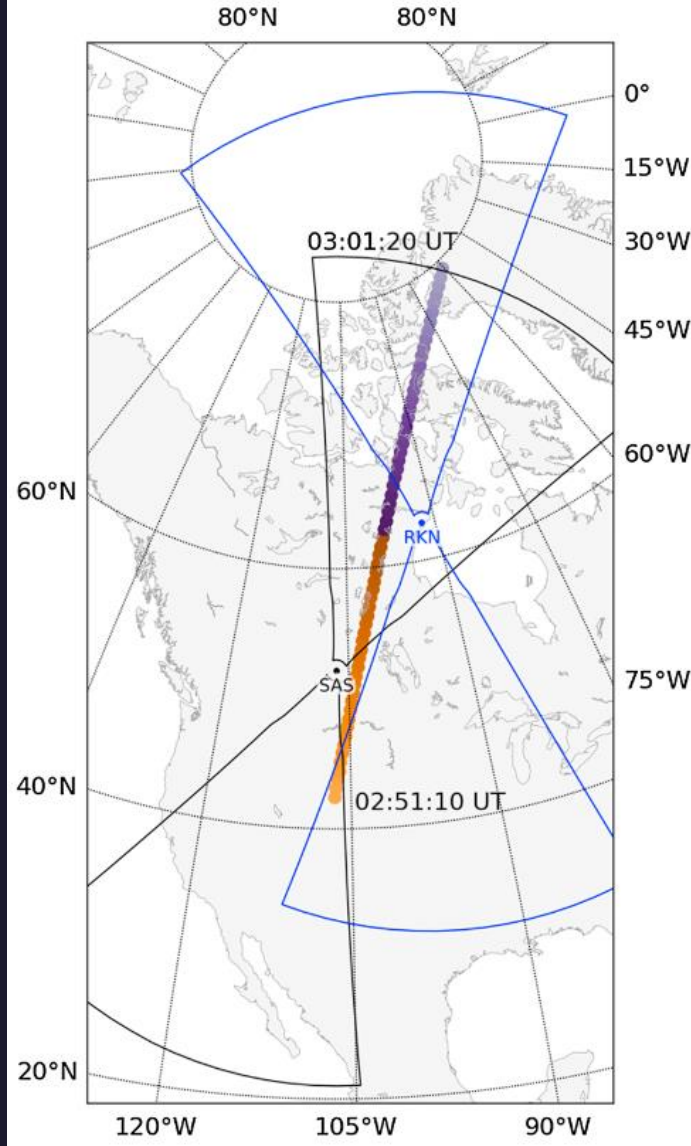
Thermospheric Density

Plasma Structure

Radio Science – *VLF Wave Amplification*

Radio Science

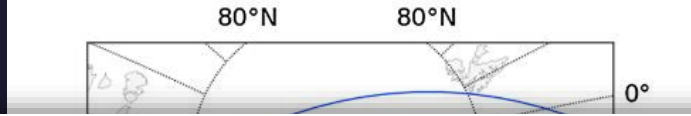
SuperDARN



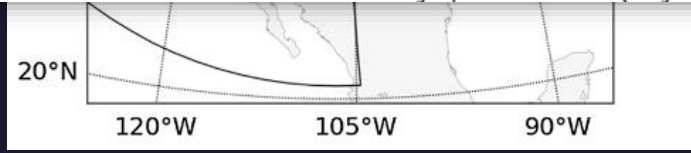
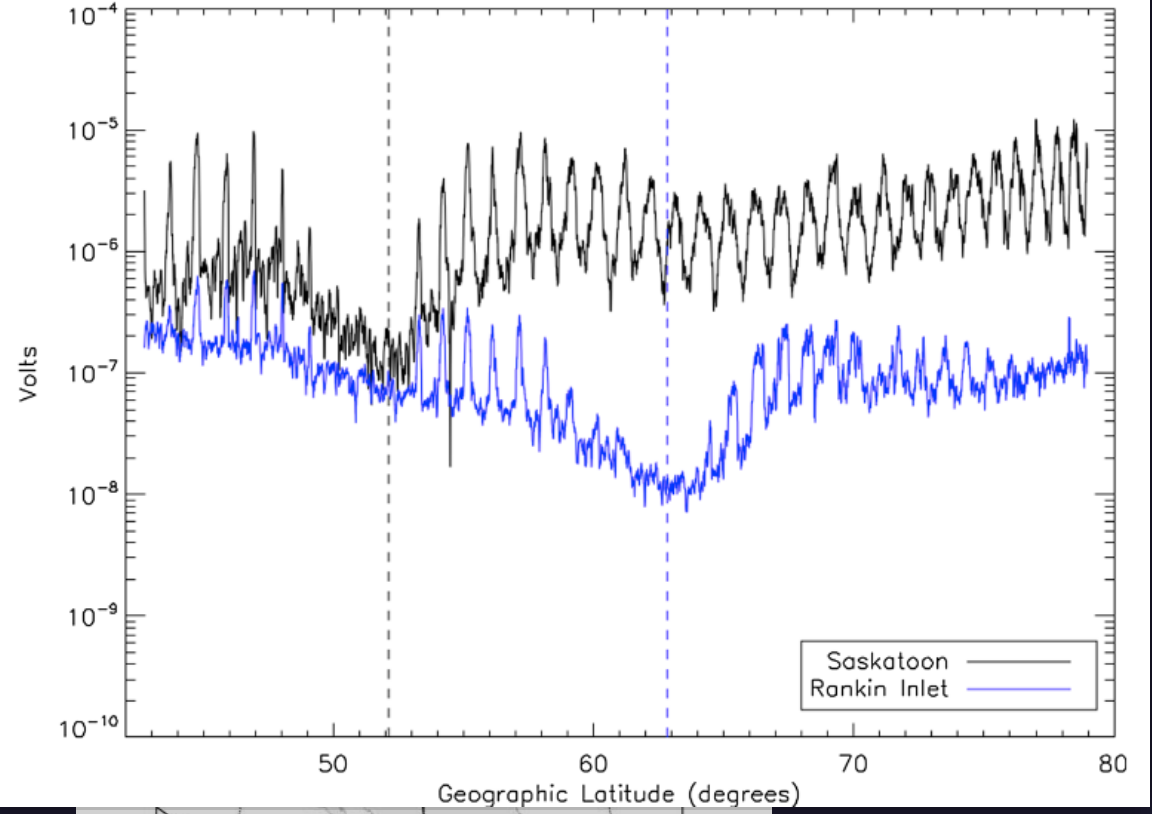
Burrell, A. G., S. E. Milan, G. W. Perry, T. K. Yeoman, and M. Lester (2015), Automatically determining the origin direction and propagation mode of high-frequency radar backscatter, *Radio Sci.*, 50, 1225–1245, doi:10.1002/2015RS005808

Radio Science

SuperDARN



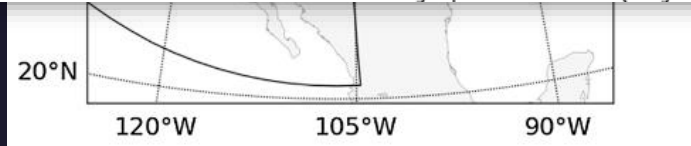
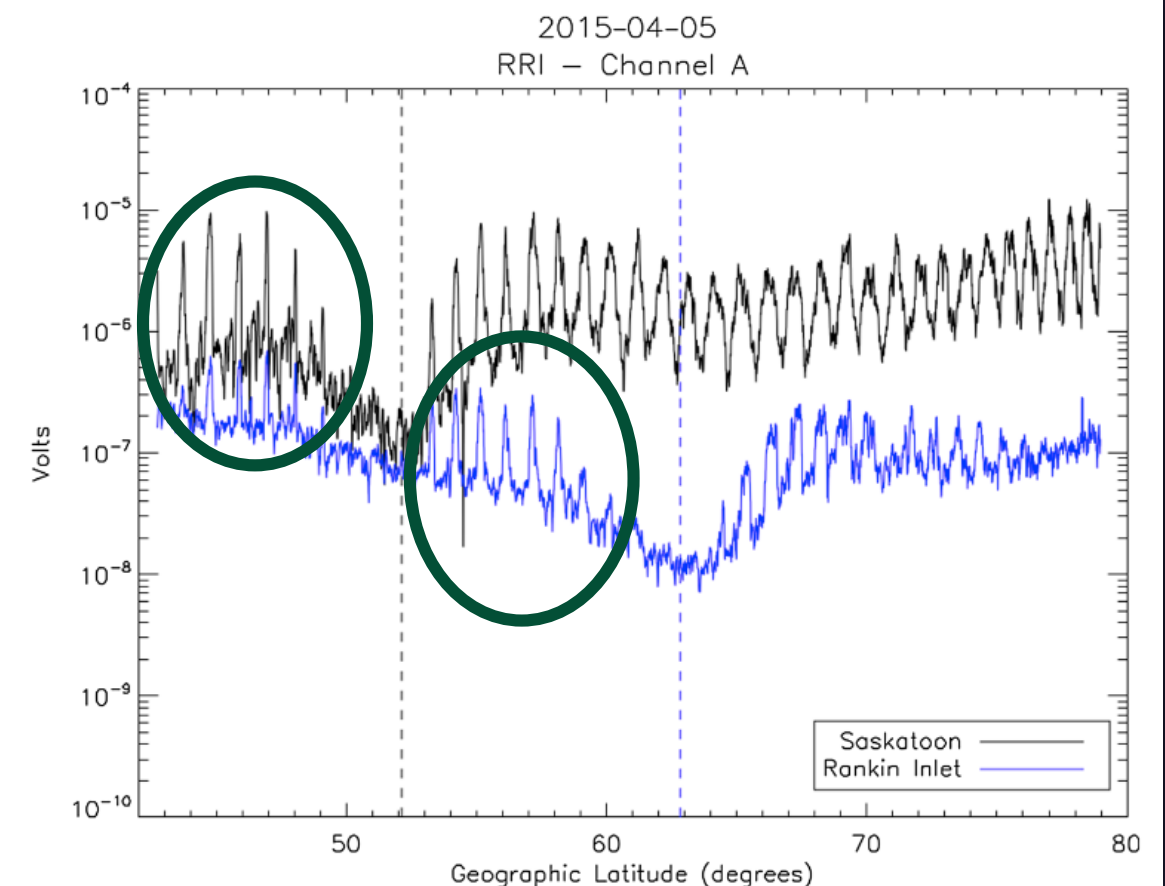
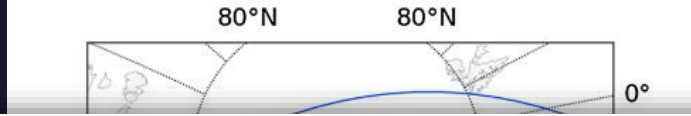
2015-04-05
RRI - Channel A



Burrell, A. G., S. E. Milan, G. W. Perry, T. K. Yeoman, and M. Lester (2015), Automatically determining the origin direction and propagation mode of high-frequency radar backscatter, *Radio Sci.*, 50, 1225–1245, doi:10.1002/2015RS005808

Radio Science

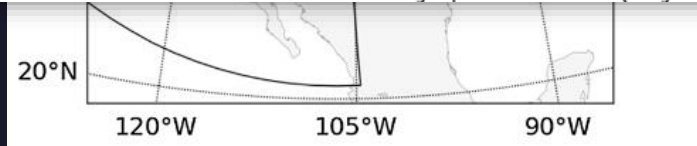
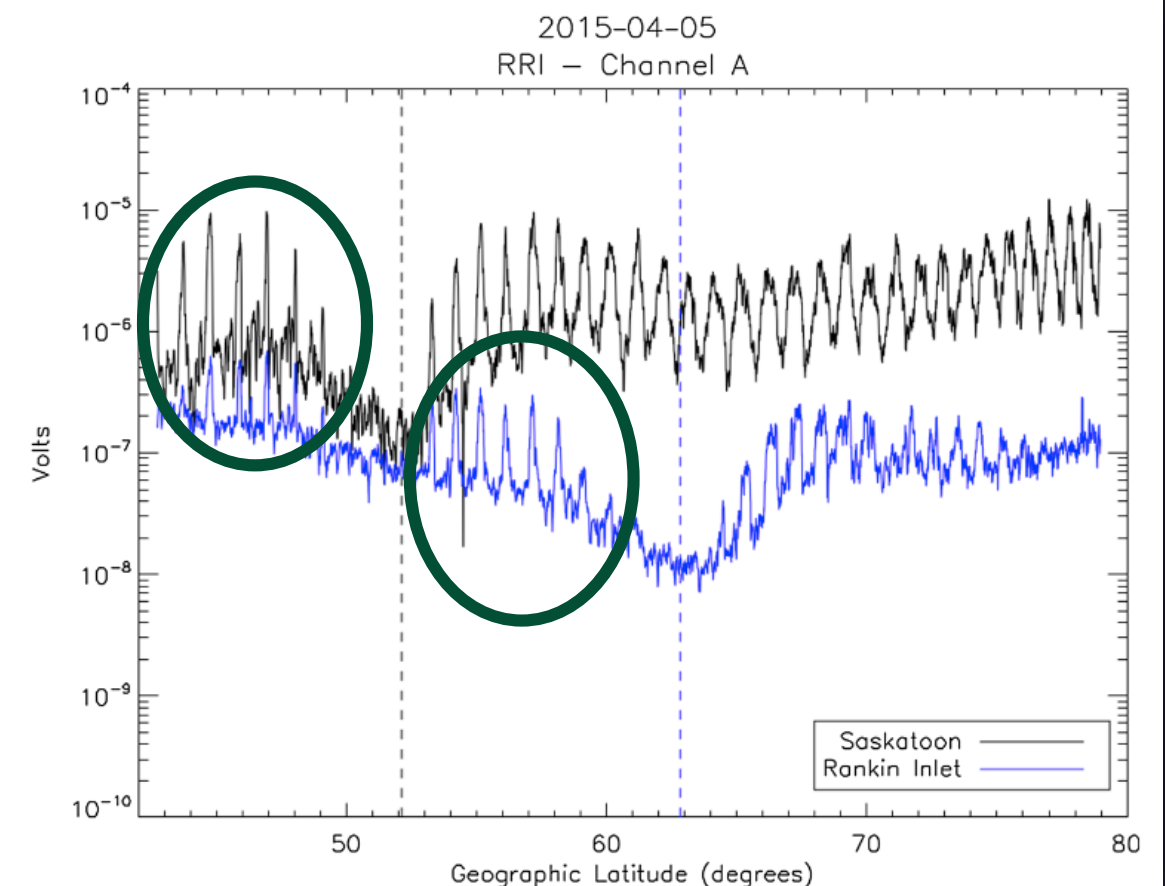
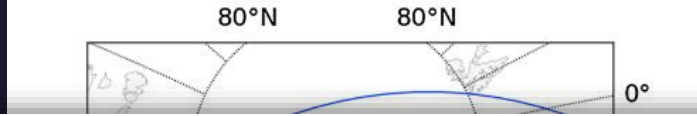
SuperDARN



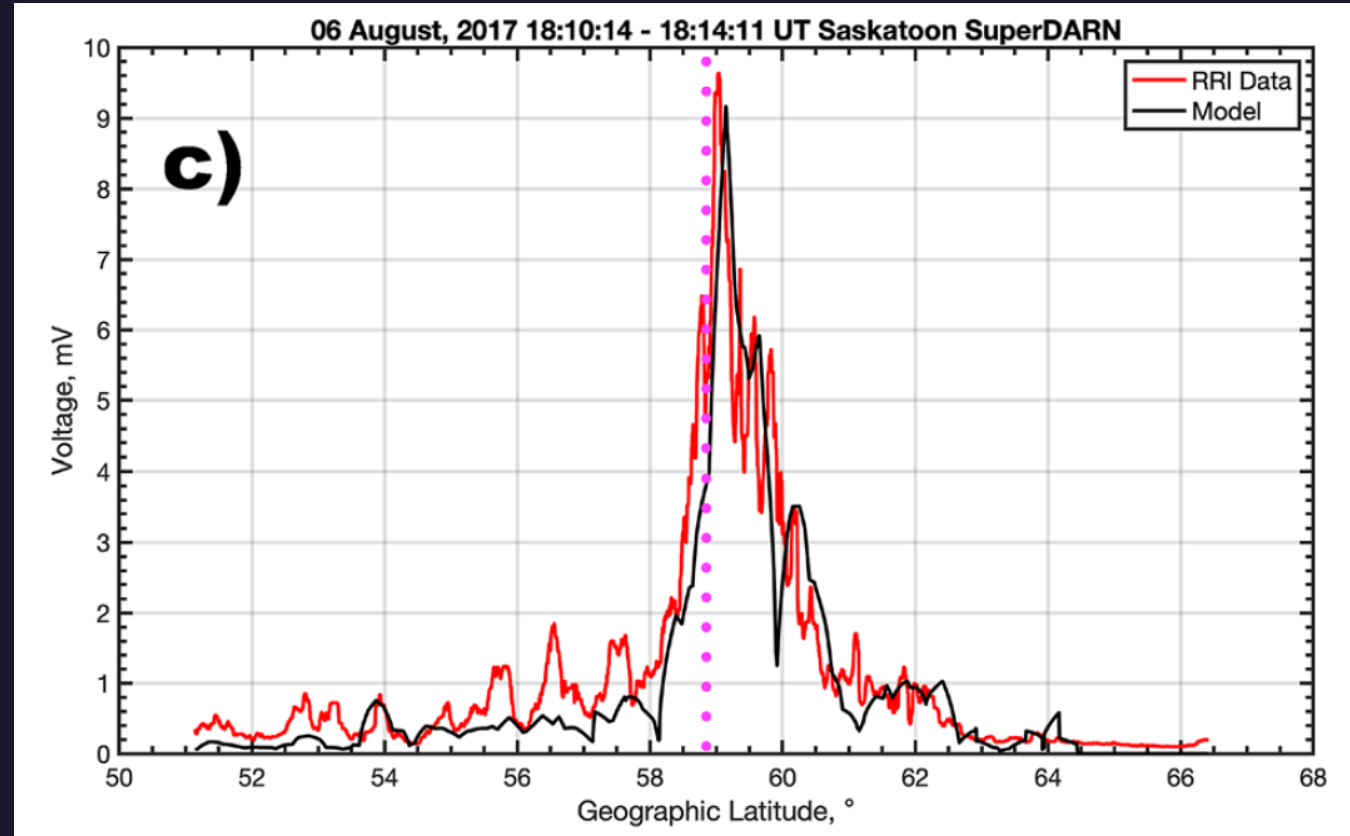
Burrell, A. G., S. E. Milan, G. W. Perry, T. K. Yeoman, and M. Lester (2015), Automatically determining the origin direction and propagation mode of high-frequency radar backscatter, *Radio Sci.*, 50, 1225–1245, doi:10.1002/2015RS005808

Radio Science

SuperDARN

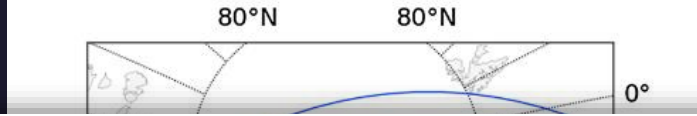


Modeling SuperDARN signals



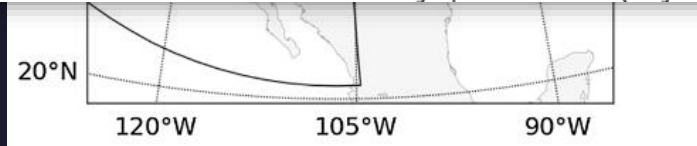
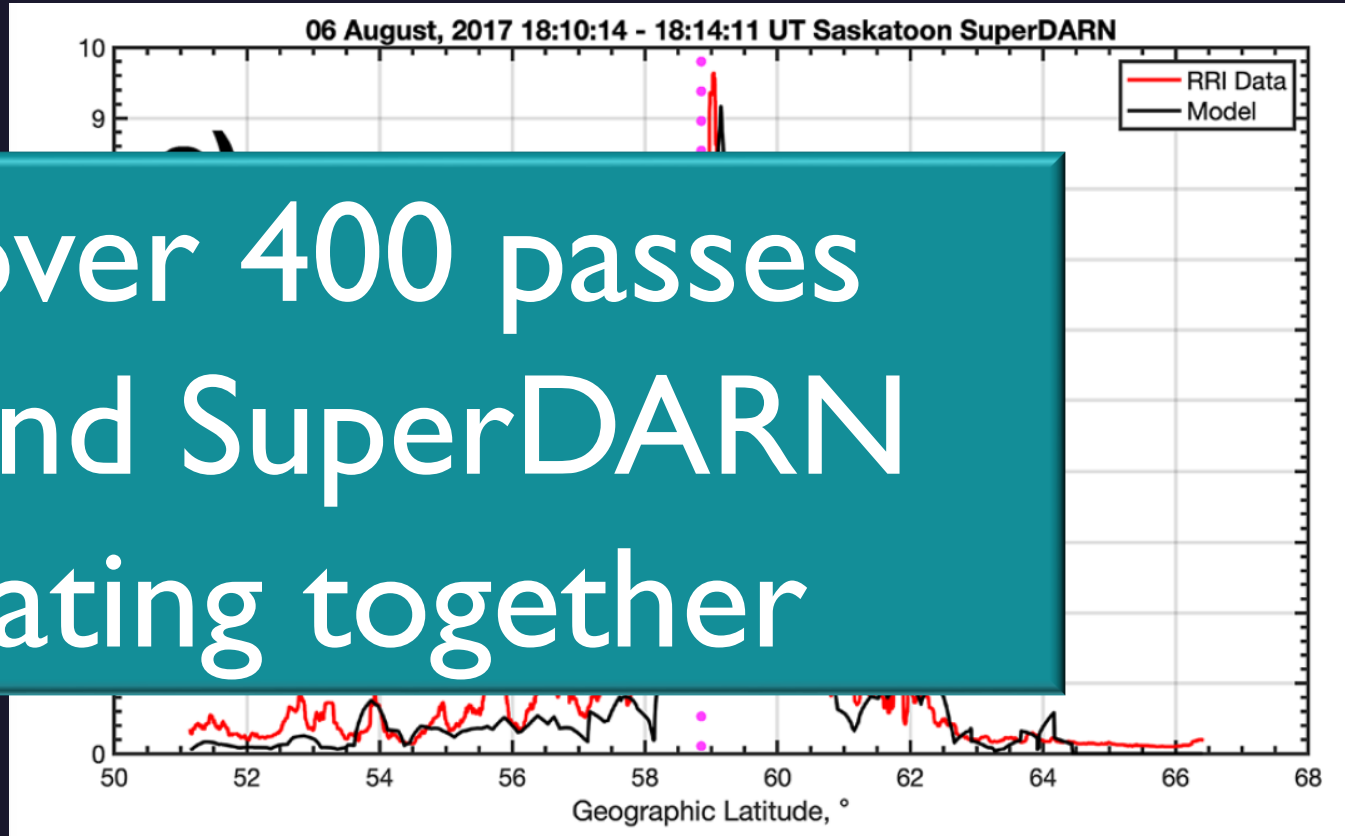
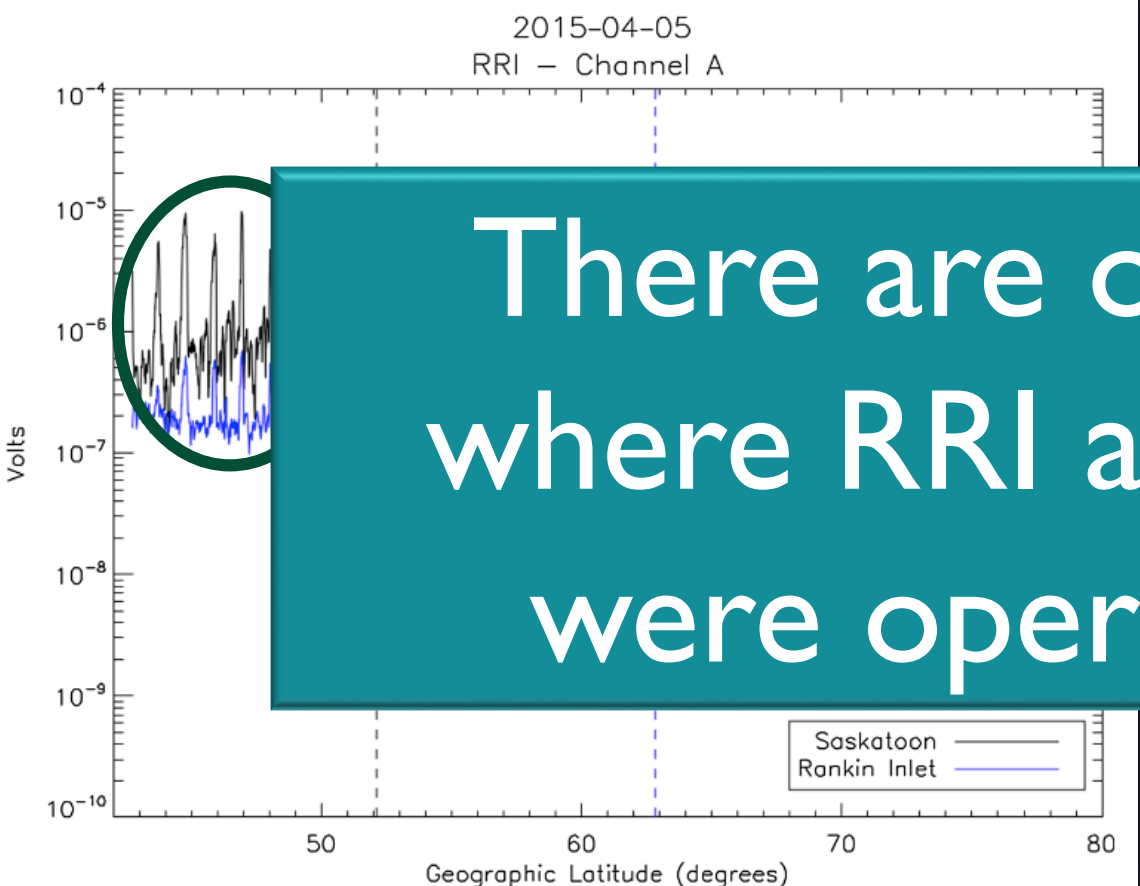
Perry, G. W., Ruzic, K. D., Sterne, K., Howarth, A. D., & Yau, A. W. (2022). Modeling and validating a SuperDARN radar's Poynting flux profile. *Radio Science*, 57, e2021RS007323. <https://doi.org/10.1029/2021RS007323>

Burrell, A. G., S. E. Milan, G. W. Perry, T. K. Yeoman, and M. Lester (2015), Automatically determining the origin direction and propagation mode of high-frequency radar backscatter, *Radio Sci.*, 50, 1225–1245, doi:10.1002/2015RS005808



Modeling SuperDARN signals

There are over 400 passes where RRI and SuperDARN were operating together

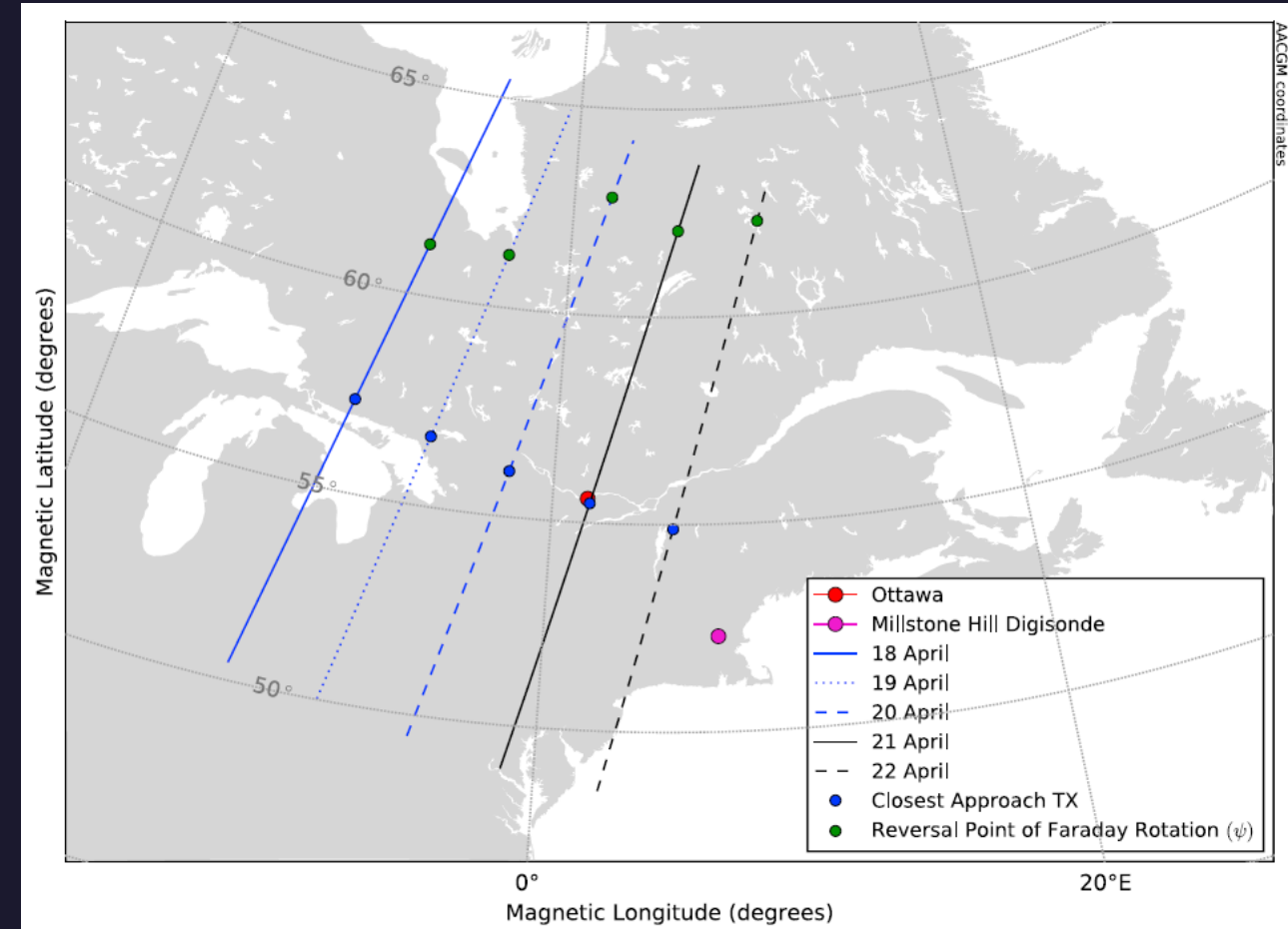


Perry, G. W., Ruzic, K. D., Sterne, K., Howarth, A. D., & Yau, A. W. (2022). Modeling and validating a SuperDARN radar's Poynting flux profile. *Radio Science*, 57, e2021RS007323. <https://doi.org/10.1029/2021RS007323>

Burrell, A. G., S. E. Milan, G. W. Perry, T. K. Yeoman, and M. Lester (2015), Automatically determining the origin direction and propagation mode of high-frequency radar backscatter, *Radio Sci.*, 50, 1225–1245, doi:10.1002/2015RS005808



- NRCan HF transmitter at Ottawa
 - CW and BPSK Modulation
- Over 50 coordinated passes
- Characteristics of wave propagation
 - Faraday rotation
 - Polarization
 - O-mode vs X-mode propagation



Danskin, D. W., Hussey, G. C., Gillies, R. G., James, H. G., Fairbairn, D. T., & Yau, A. W. (2018). Polarization characteristics inferred from the Radio Receiver Instrument on the enhanced Polar Outflow Probe. *Journal of Geophysical Research: Space Physics*, 123, 1648–1662.

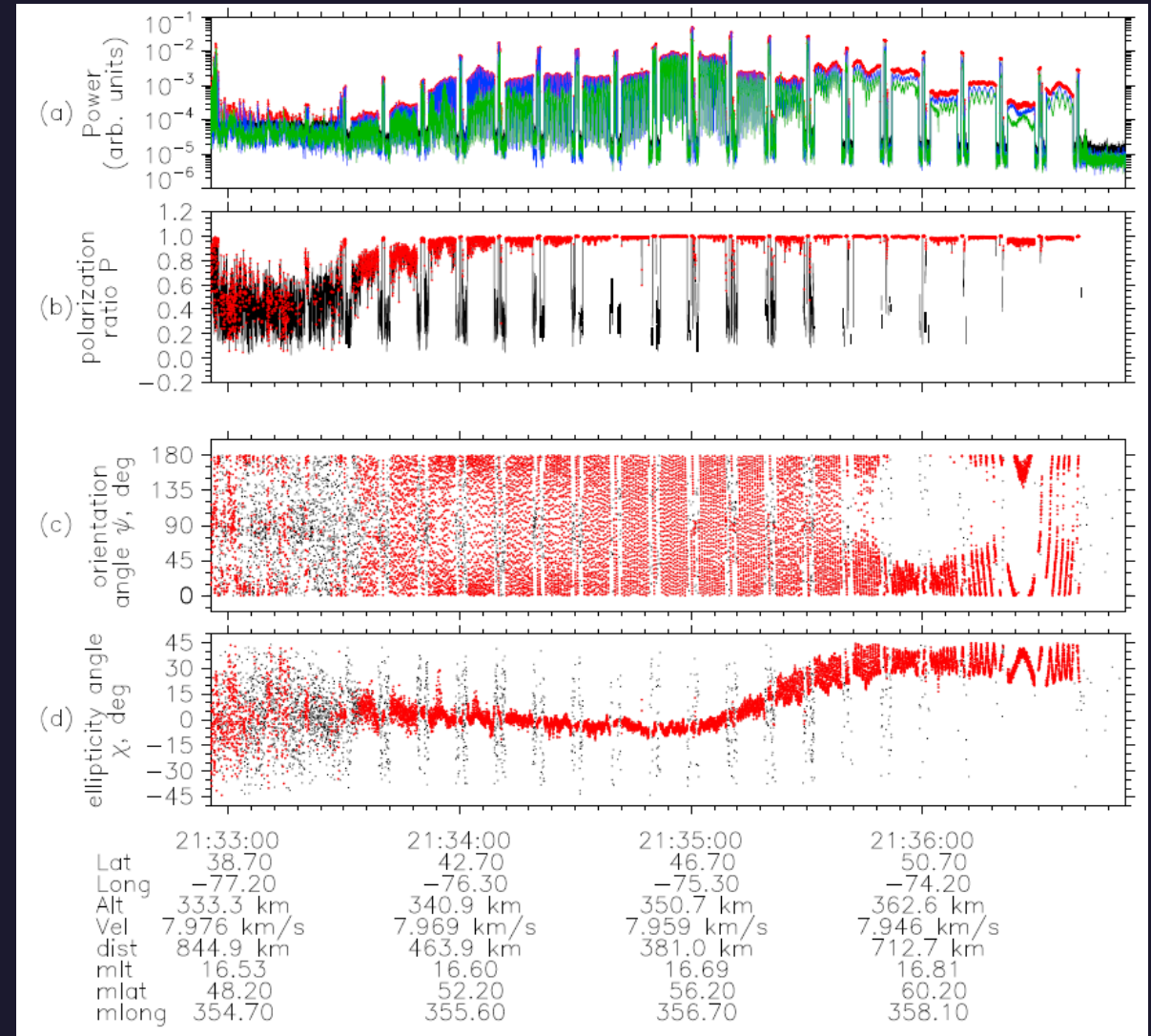
<https://doi.org/10.1002/2017JA024731>

Radio Science

HF Propagation



- NRCan HF transmitter at Ottawa
 - CW and BPSK Modulation
- Over 50 coordinated passes
- Characteristics of wave propagation
 - Faraday rotation
 - Polarization
 - O-mode vs X-mode propagation

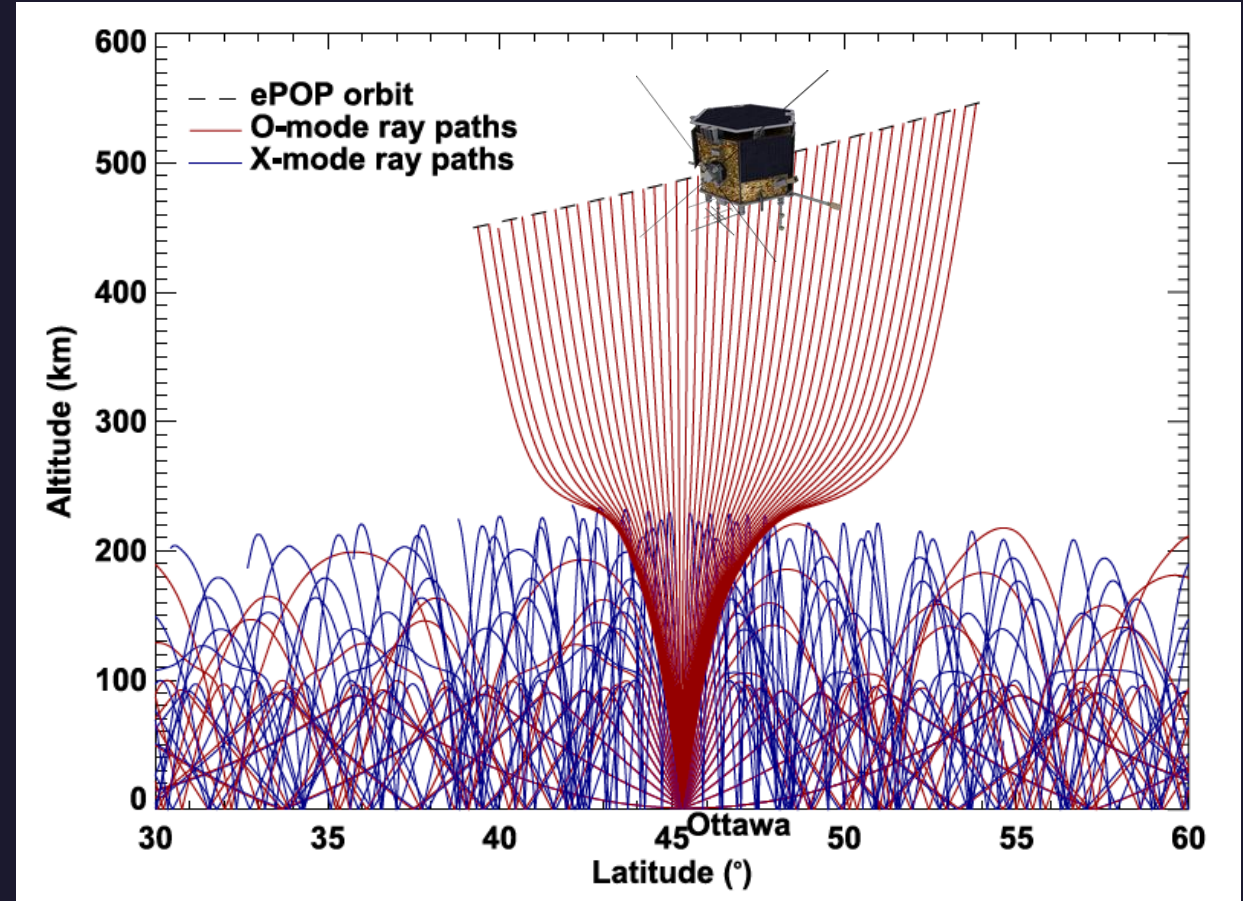


Danskin, D. W., Hussey, G. C., Gillies, R. G., James, H. G., Fairbairn, D. T., & Yau, A. W. (2018). Polarization characteristics inferred from the Radio Receiver Instrument on the enhanced Polar Outflow Probe. *Journal of Geophysical Research: Space Physics*, 123, 1648–1662.

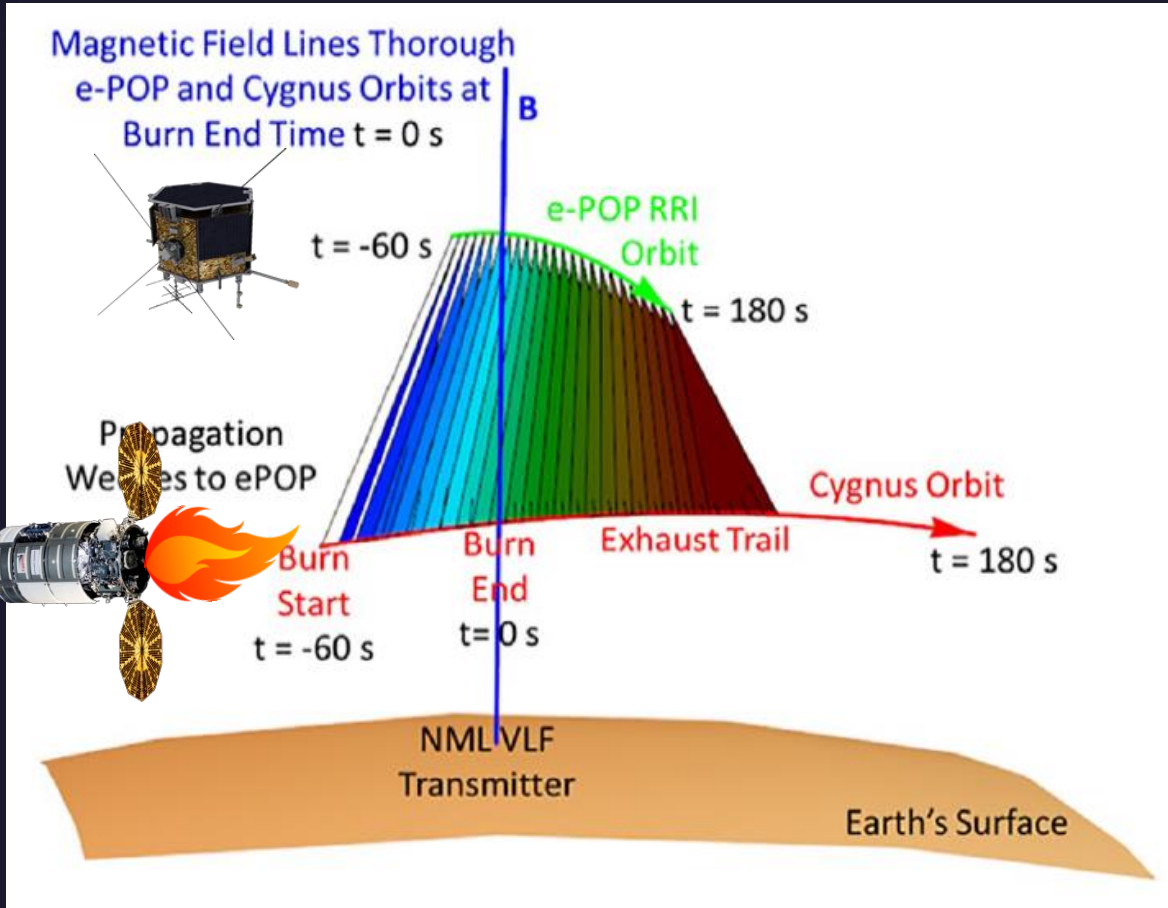
<https://doi.org/10.1002/2017JA024731>



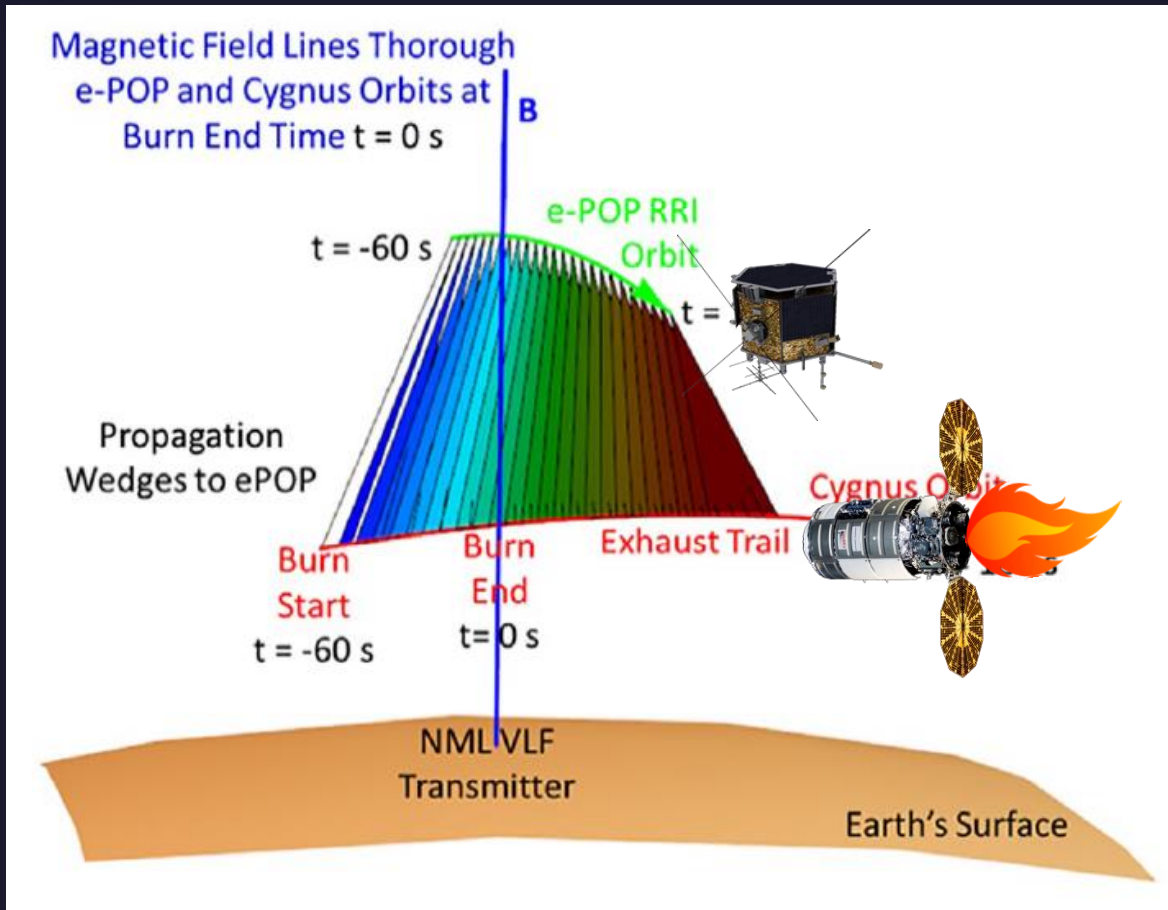
- NRCan HF transmitter at Ottawa
 - CW and BPSK Modulation
- Over 50 coordinated passes
- Characteristics of wave propagation
 - Faraday rotation
 - Polarization
 - O-mode vs X-mode propagation



Pandey, K., Eyiguler, E. C. K., Gillies, R. G., Hussey, G. C., Danskin, D. W., & Yau, A. W. (2022). Polarization characteristics of a single mode radio wave traversing through the ionosphere: A unique observation from the RRI on ePOP/SWARM-E. *Journal of Geophysical Research: Space Physics*, 127, e2022JA030684. <https://doi.org/10.1029/2022JA030684>



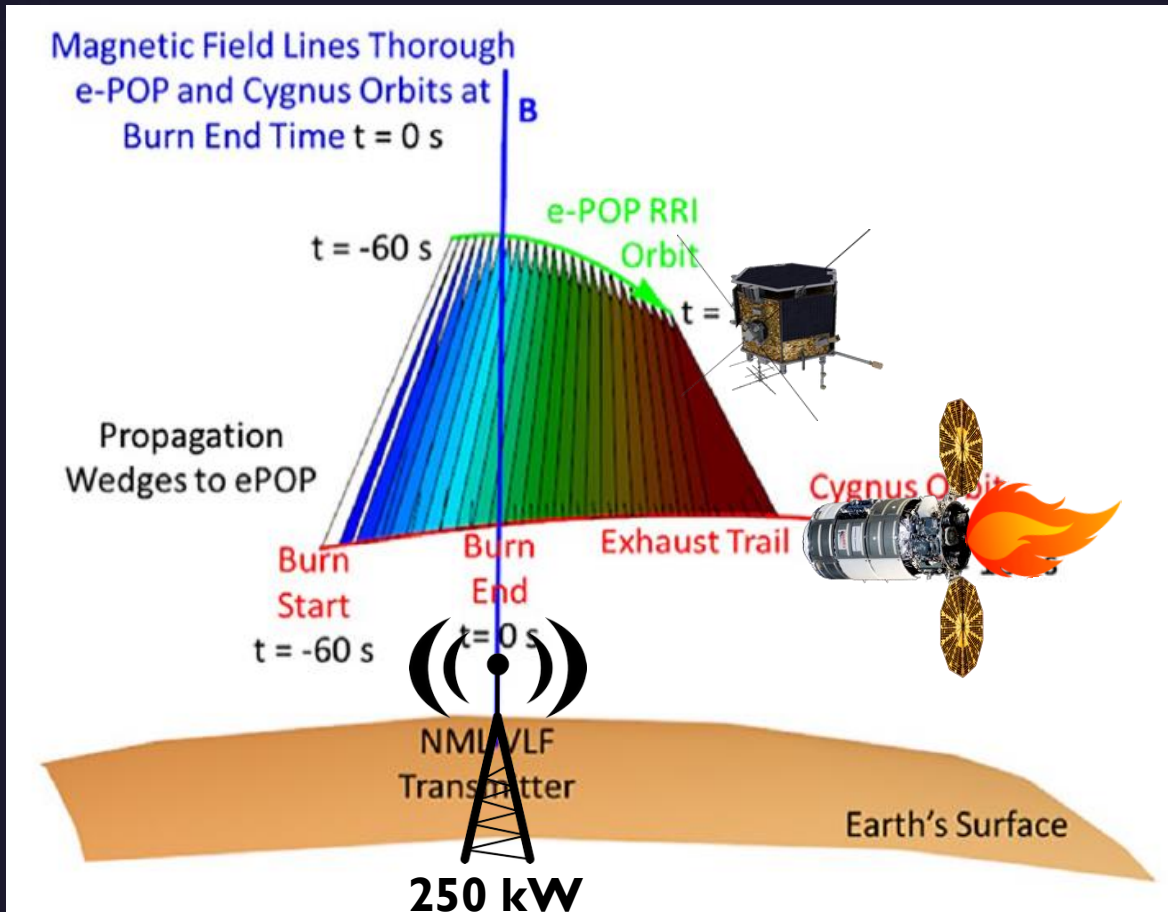
Bernhardt, P. A., Bougas, W. C., Griffin, M. K., Watson, C., Langley, R. B., Howarth, A. D., et al. (2021). Strong amplification of ELF/VLF signals in space using neutral gas injections from a satellite rocket engine. *Radio Science*, 56, e2020RS007207. <https://doi.org/10.1029/2020RS007207>



Bernhardt, P. A., Bougas, W. C., Griffin, M. K., Watson, C., Langley, R. B., Howarth, A. D., et al. (2021). Strong amplification of ELF/VLF signals in space using neutral gas injections from a satellite rocket engine. *Radio Science*, 56, e2020RS007207. <https://doi.org/10.1029/2020RS007207>

Radio Science

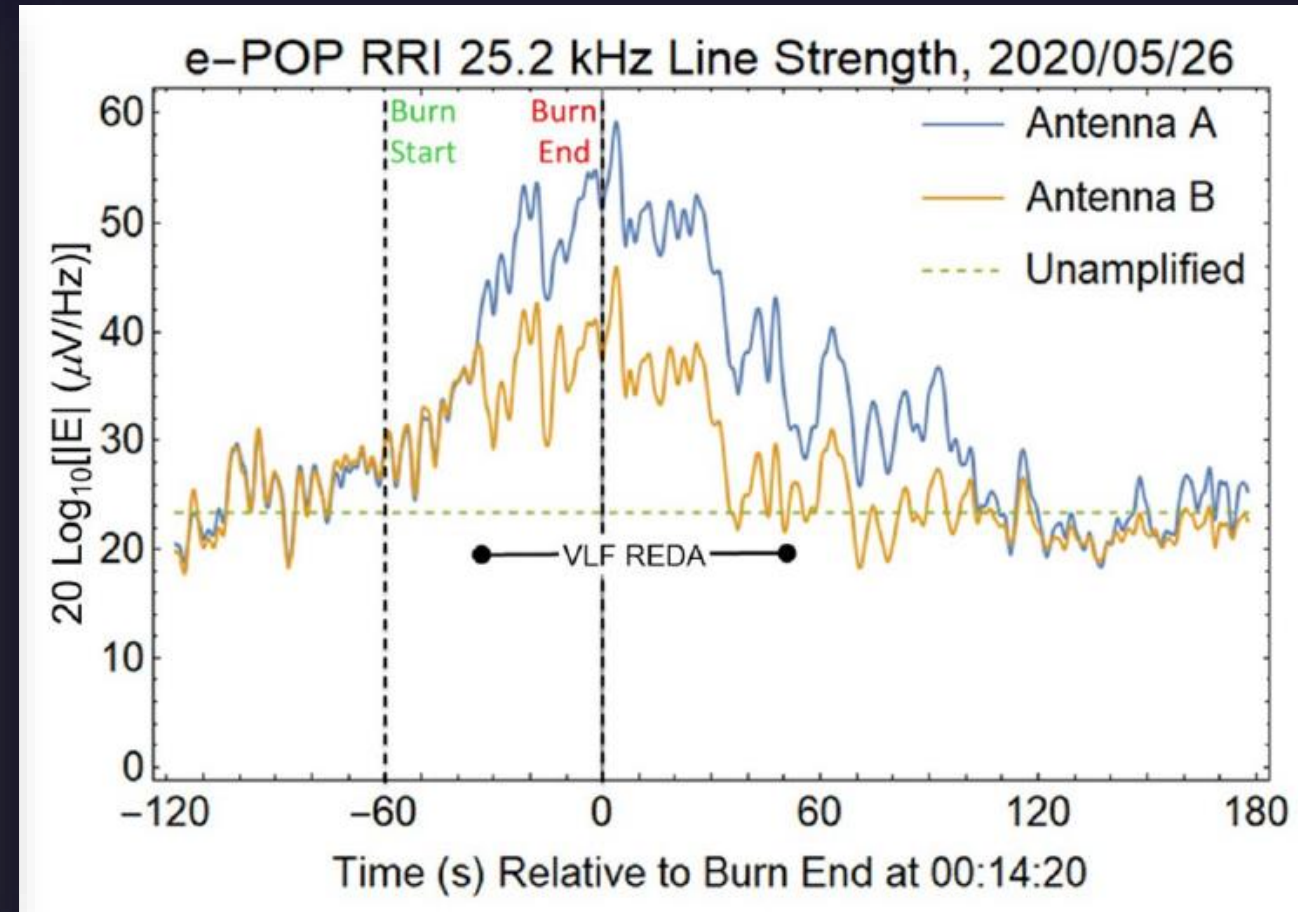
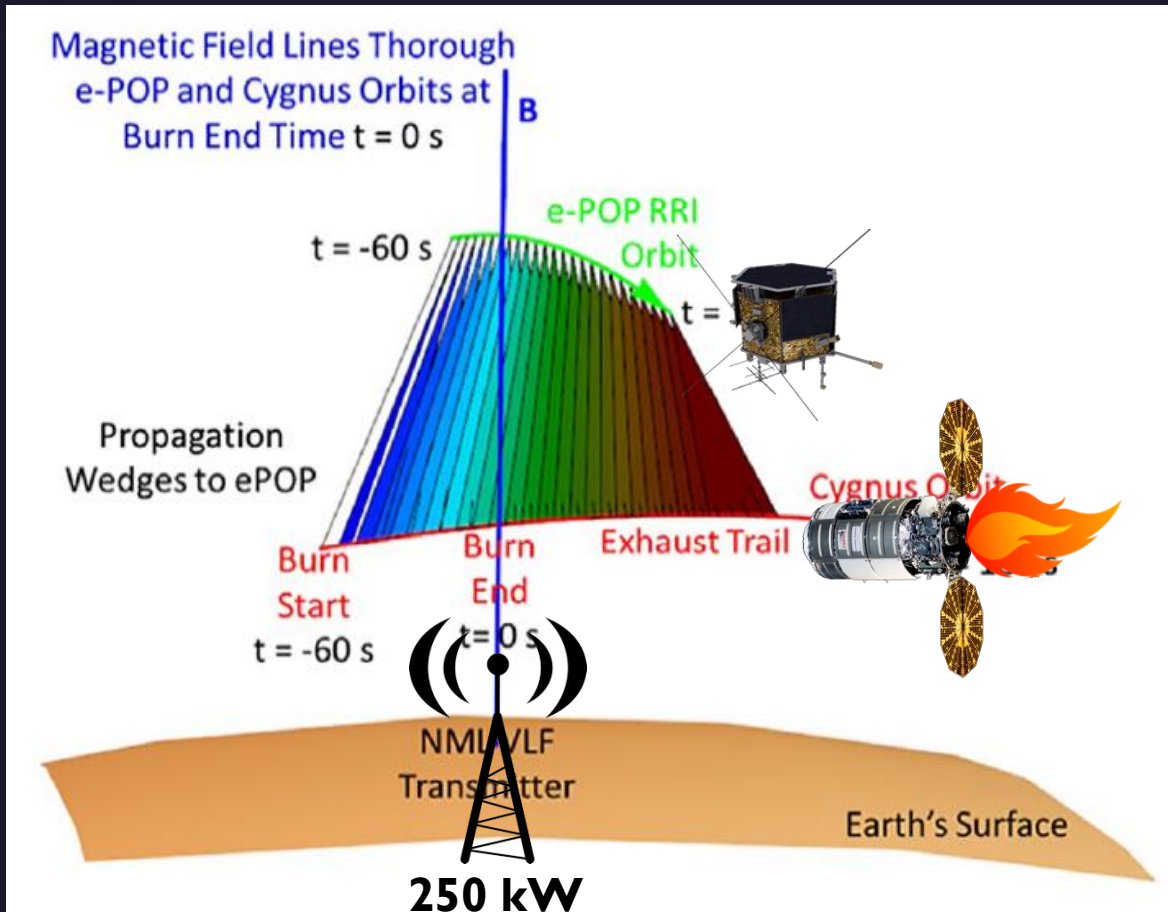
VLF Wave Amplification



Bernhardt, P. A., Bougas, W. C., Griffin, M. K., Watson, C., Langley, R. B., Howarth, A. D., et al. (2021). Strong amplification of ELF/VLF signals in space using neutral gas injections from a satellite rocket engine. *Radio Science*, 56, e2020RS007207. <https://doi.org/10.1029/2020RS007207>

Radio Science

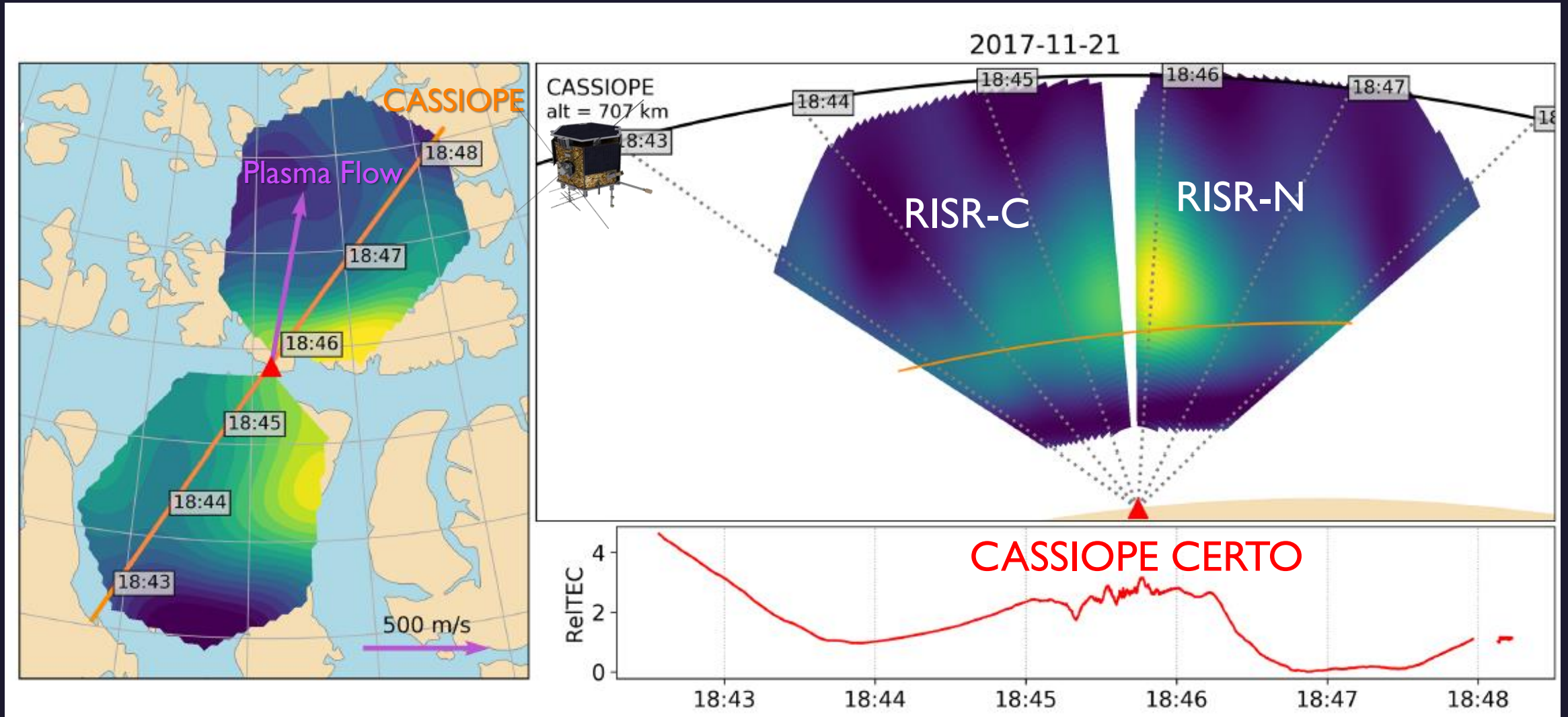
VLF Wave Amplification



Bernhardt, P. A., Bougas, W. C., Griffin, M. K., Watson, C., Langley, R. B., Howarth, A. D., et al. (2021). Strong amplification of ELF/VLF signals in space using neutral gas injections from a satellite rocket engine. *Radio Science*, 56, e2020RS007207. <https://doi.org/10.1029/2020RS007207>

Plasma

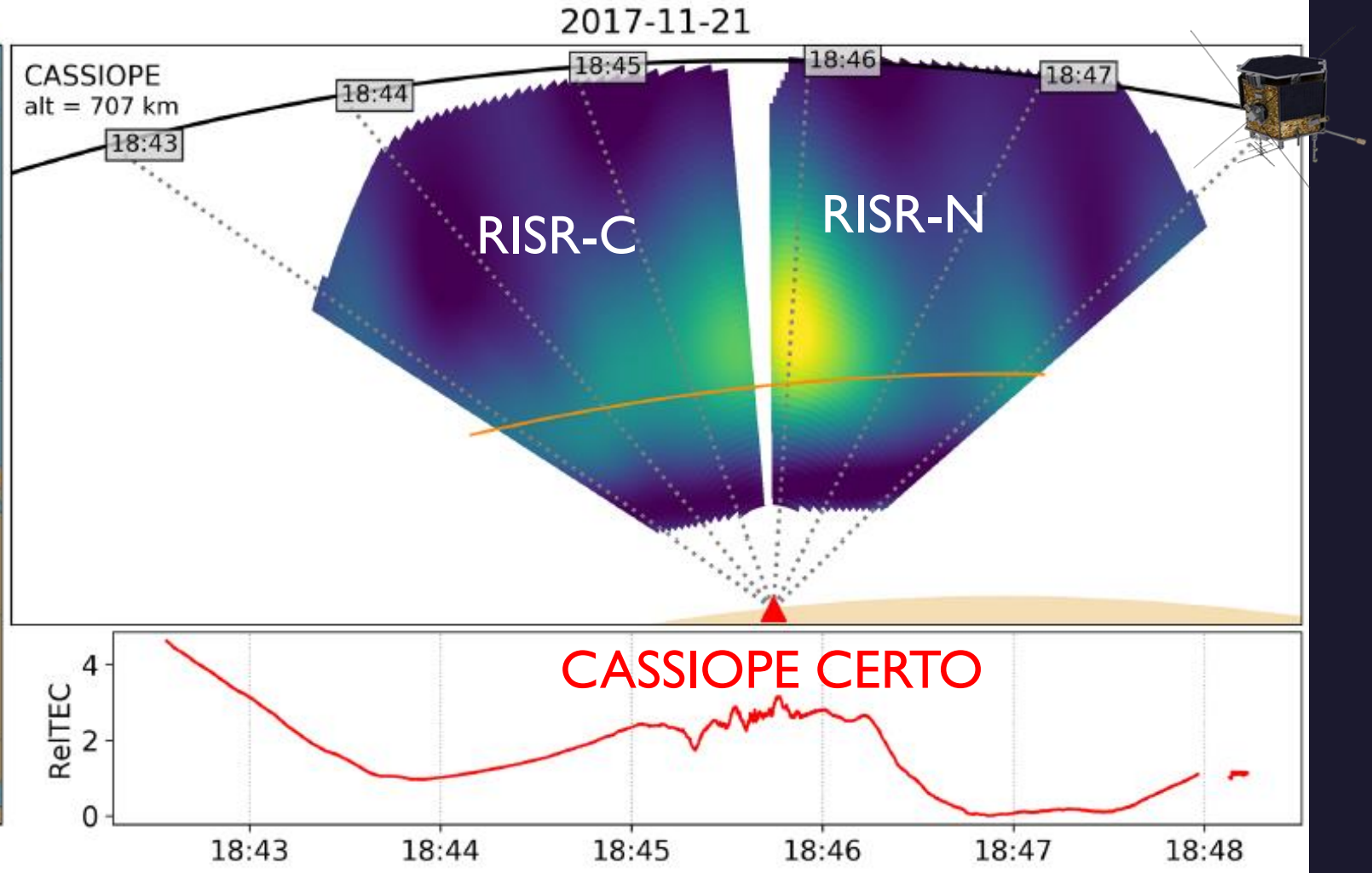
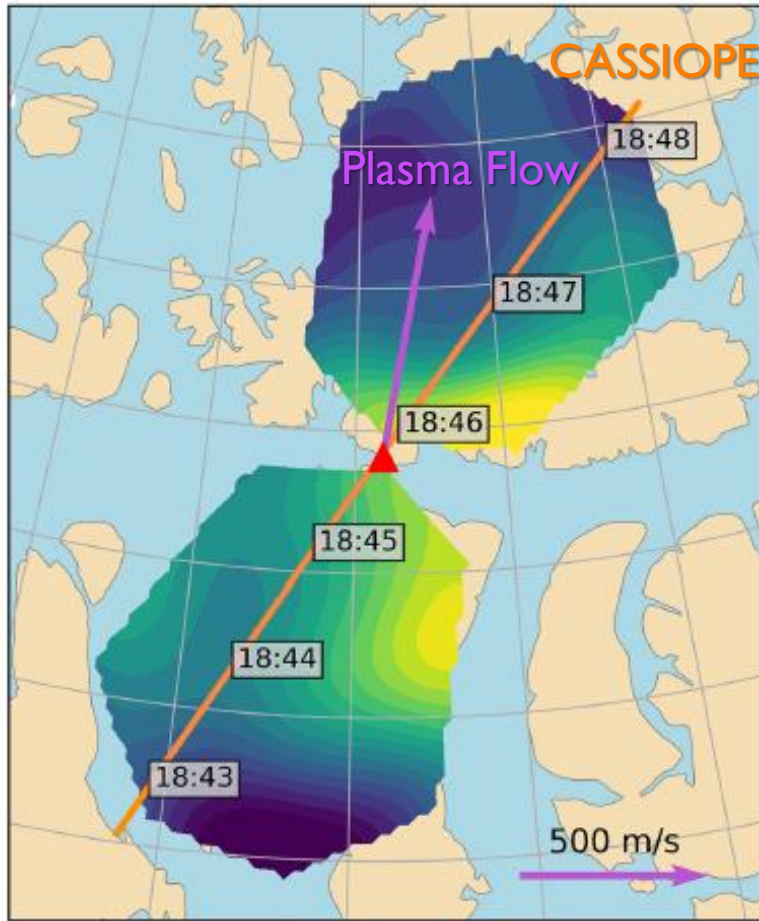
Structure



Lamarche L. J., Varney, R. H., & Siefving, C. L. (2020). Analysis of plasma irregularities on a range of scintillation-scales using the Resolute Bay Incoherent Scatter Radars. *Journal of Geophysical Research: Space Physics*, 125, e2019JA027112. <https://doi.org/10.1029/2019JA027112>

Plasma

Structure



Thermosphere

Density from GNSS



350 km Altitude

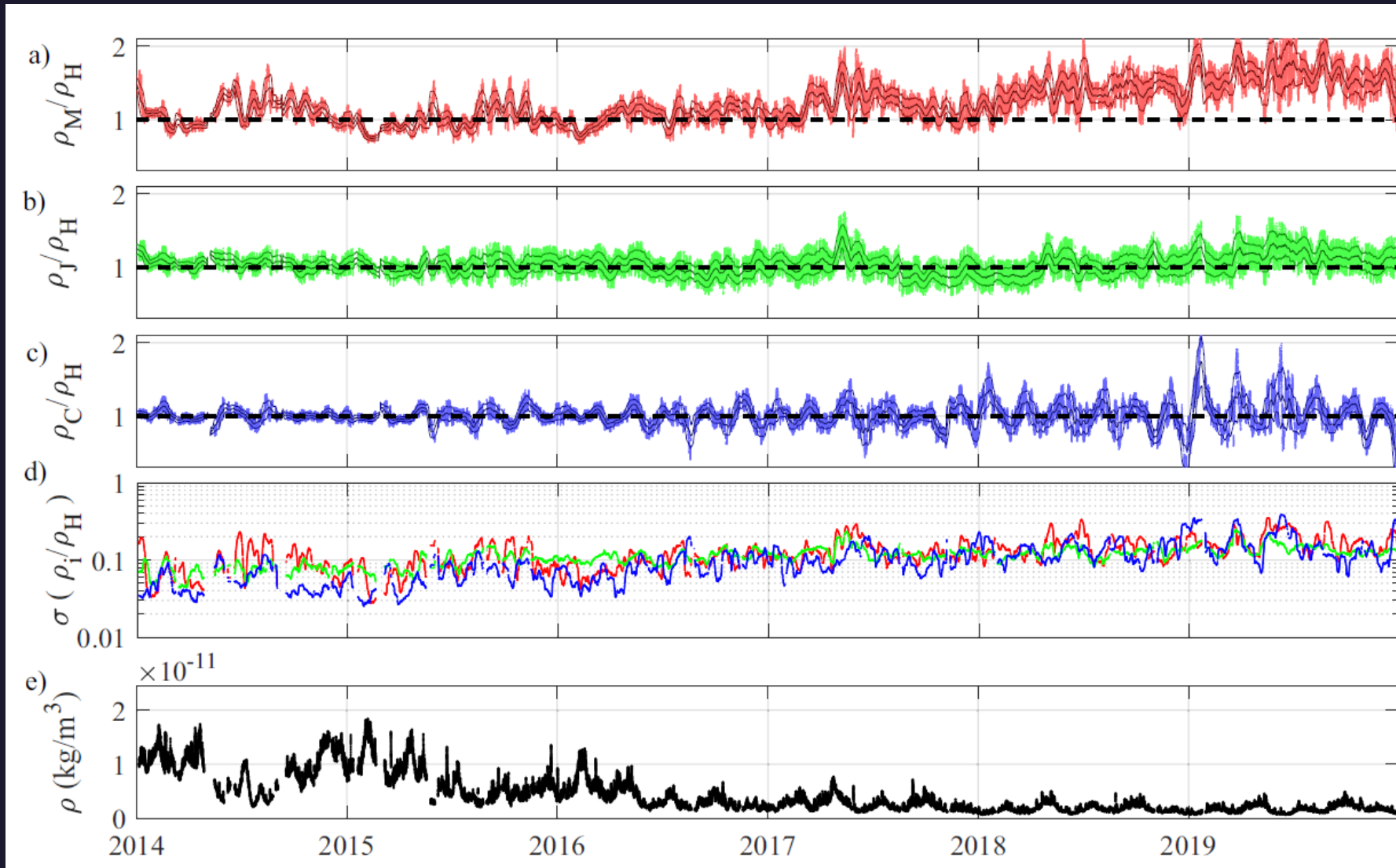
NRLMSISE-00/HASDM

JB2008/HASDM

CASSIOPE/HASDM

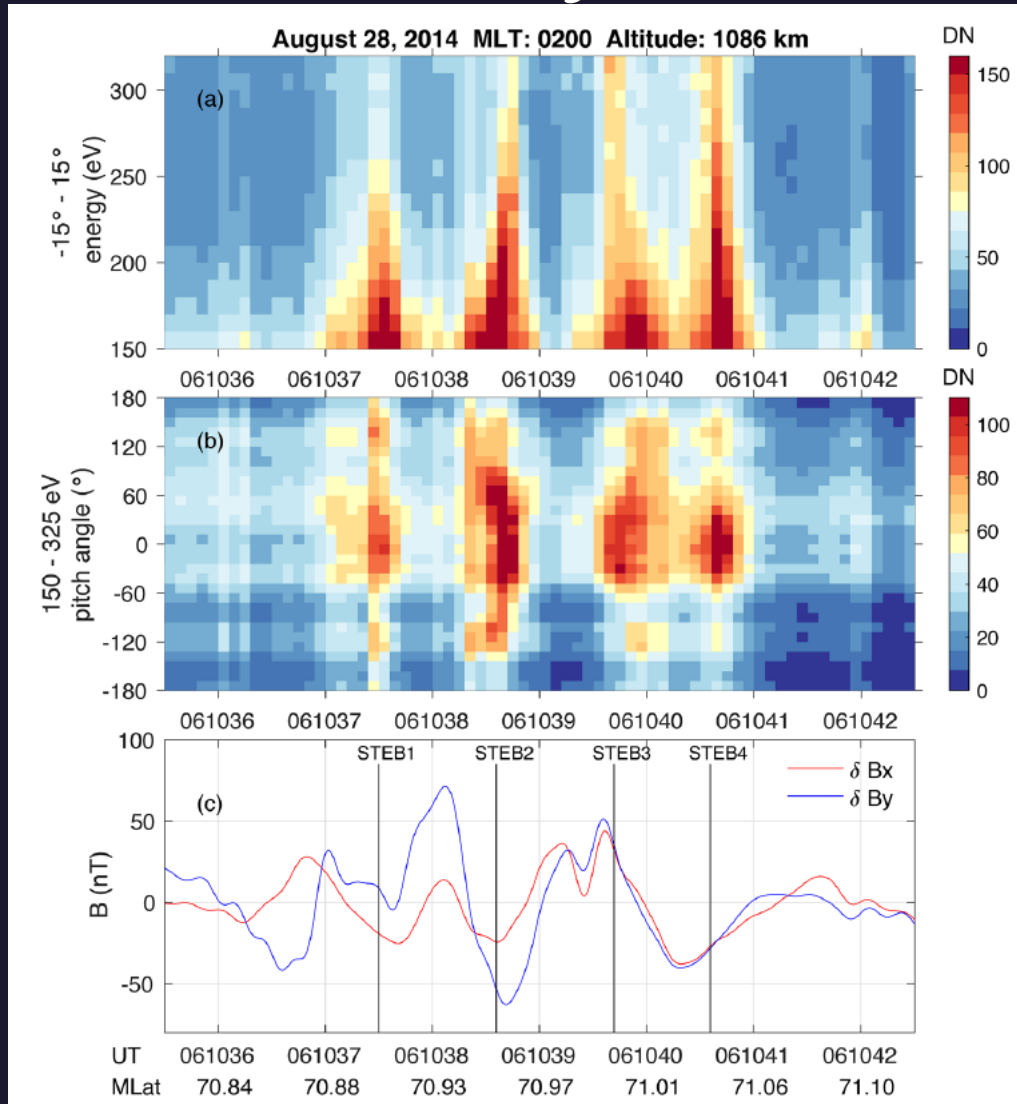
Standard Deviations

Background Density



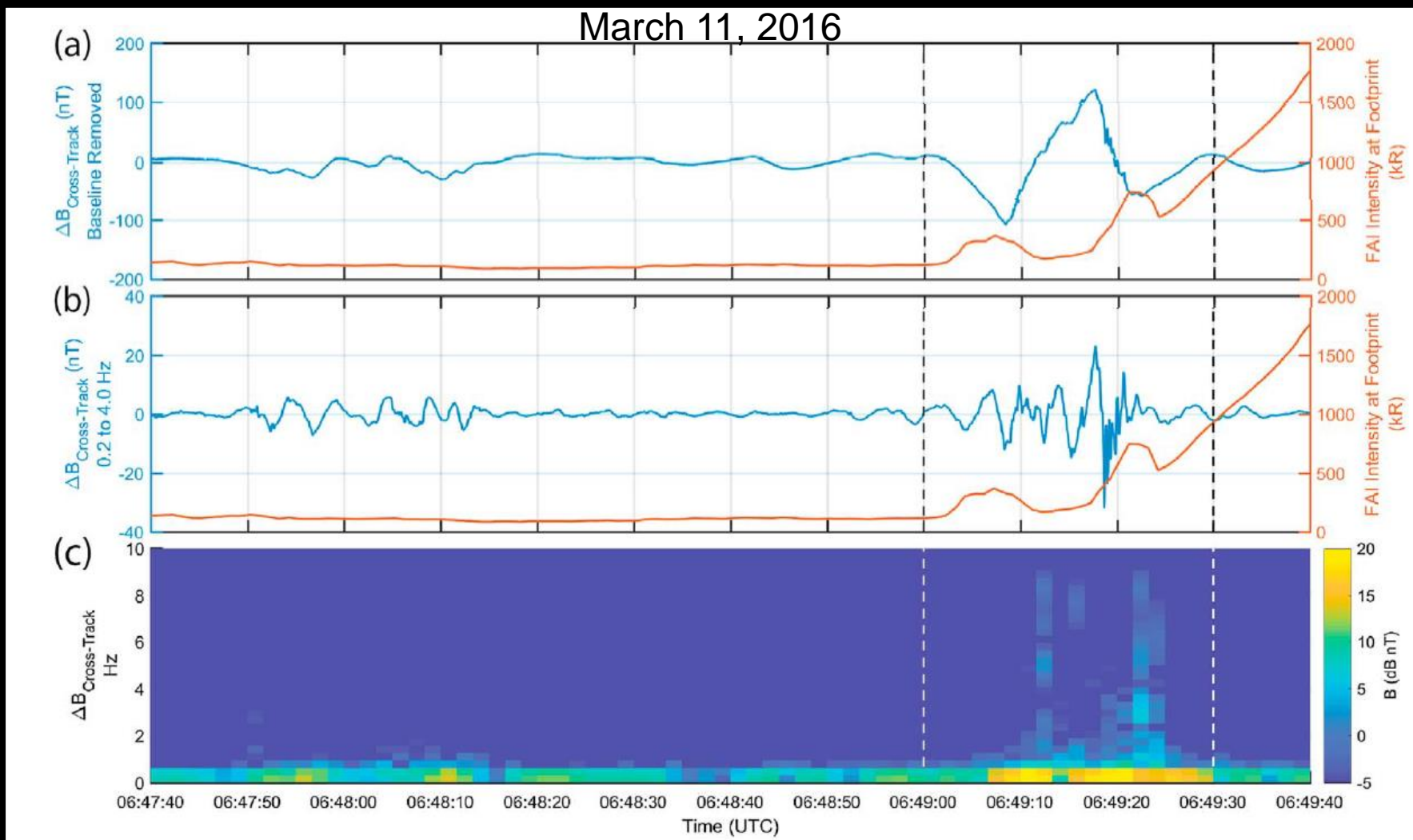
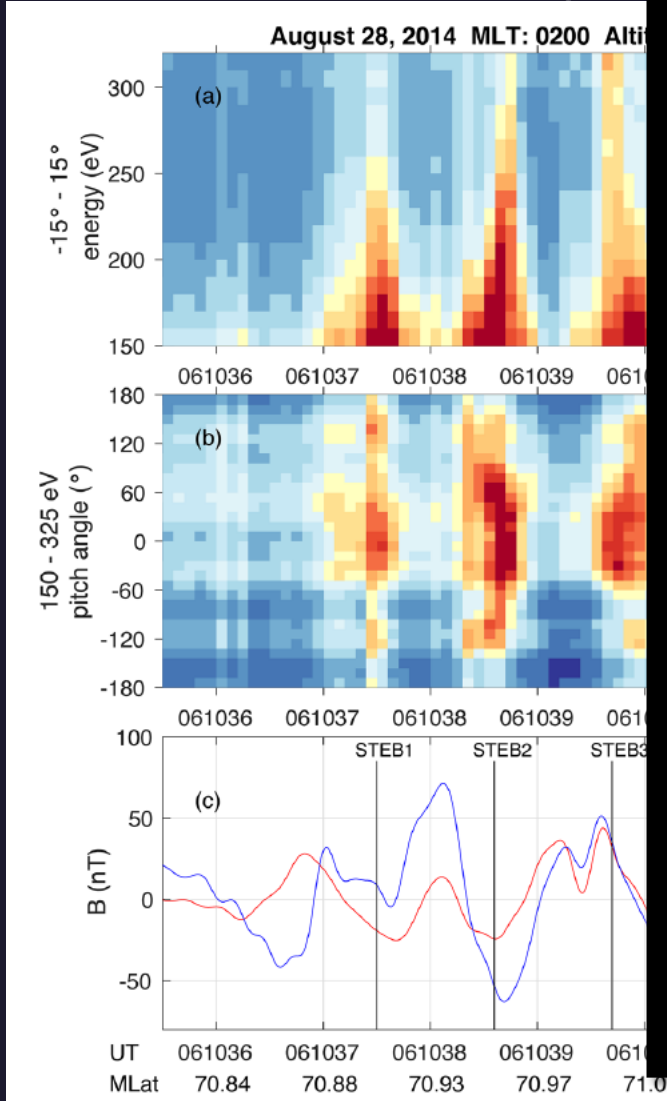
Auroral Dynamics

Alfvén Resonator



Wu, J., Knudsen, D. J., Shen, Y., & Gillies, D. M. (2021). e-POP observations of Suprathermal electron bursts in the ionospheric Alfvén resonator. *Journal of Geophysical Research: Space Physics*, 126, e2020JA028005. <https://doi.org/10.1029/2020JA028005>

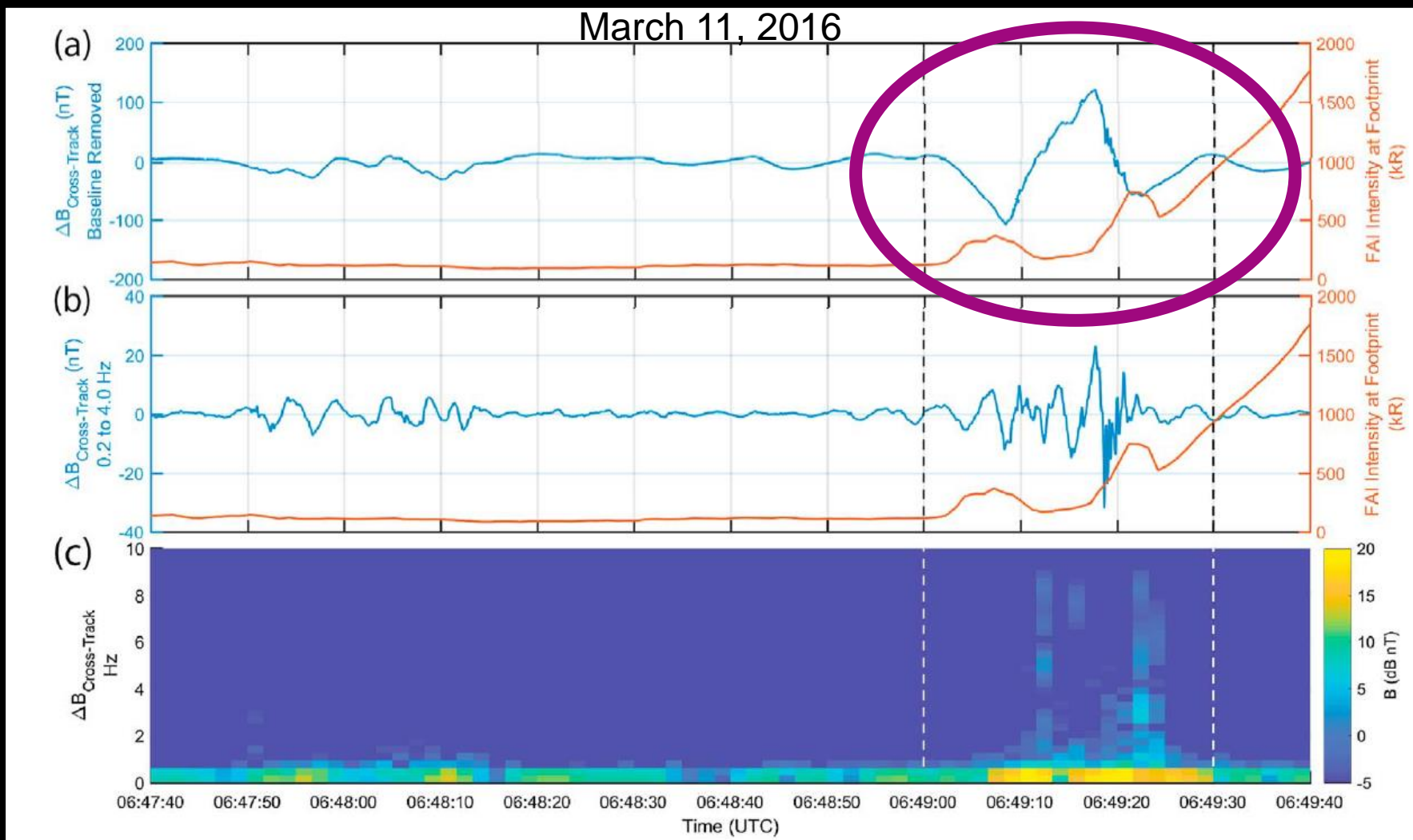
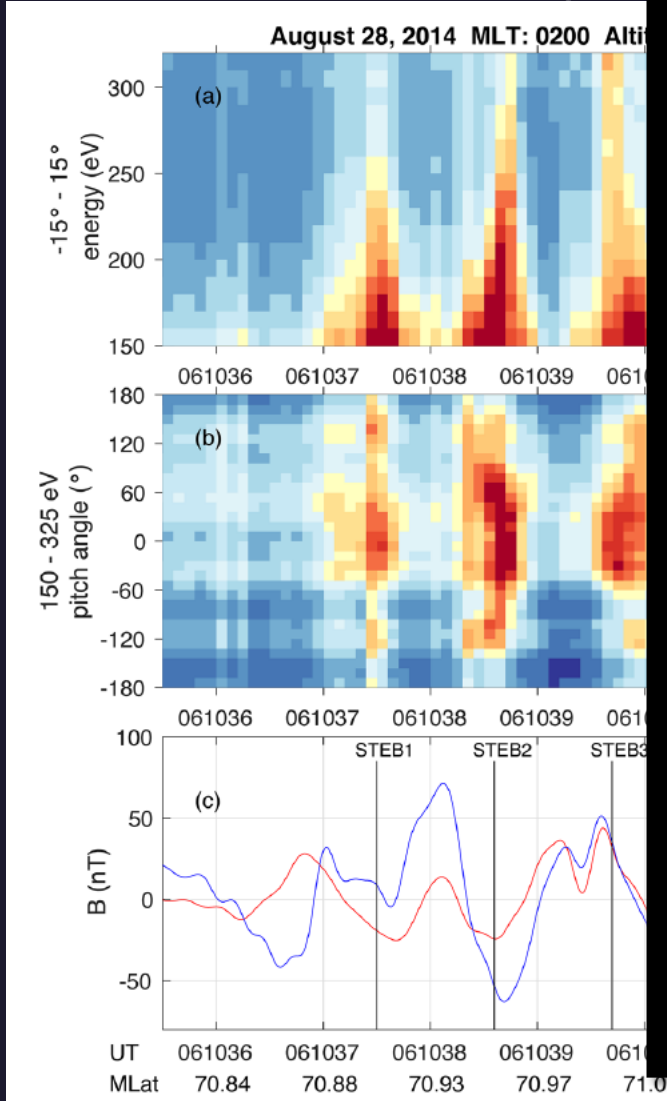
Auroral Dynamics *Alfvén Resonator*



Wu, J., Knudsen, D. J., Shen, Y., & Gillies, D. M. (2021). e-POP observations of Suprathermal electron bursts in the ionospheric Alfvén resonator. *Journal of Geophysical Research: Space Physics*, 126, e2020JA028005. <https://doi.org/10.1029/2020JA028005>

Miles, D. M., Mann, I. R., Pakhotin, I. P., Burchill, J. K., Howarth, A. D., Knudsen, D. J., ... Yau, A. W. (2018). Alfvénic dynamics and fine structuring of discrete auroral arcs: Swarm and e-POP observations. *Geophysical Research Letters*, 45. <https://doi.org/10.1002/2017GL076051>

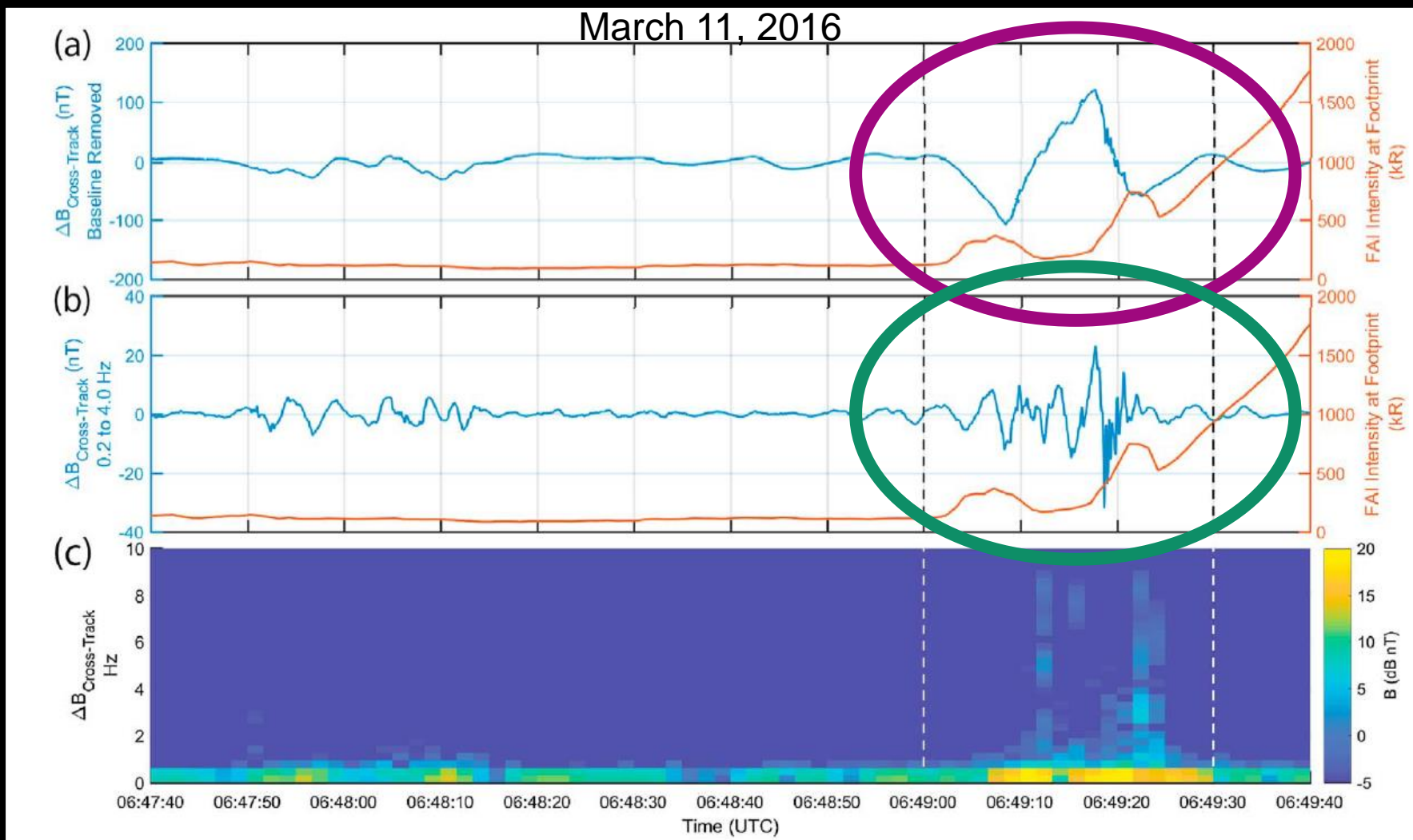
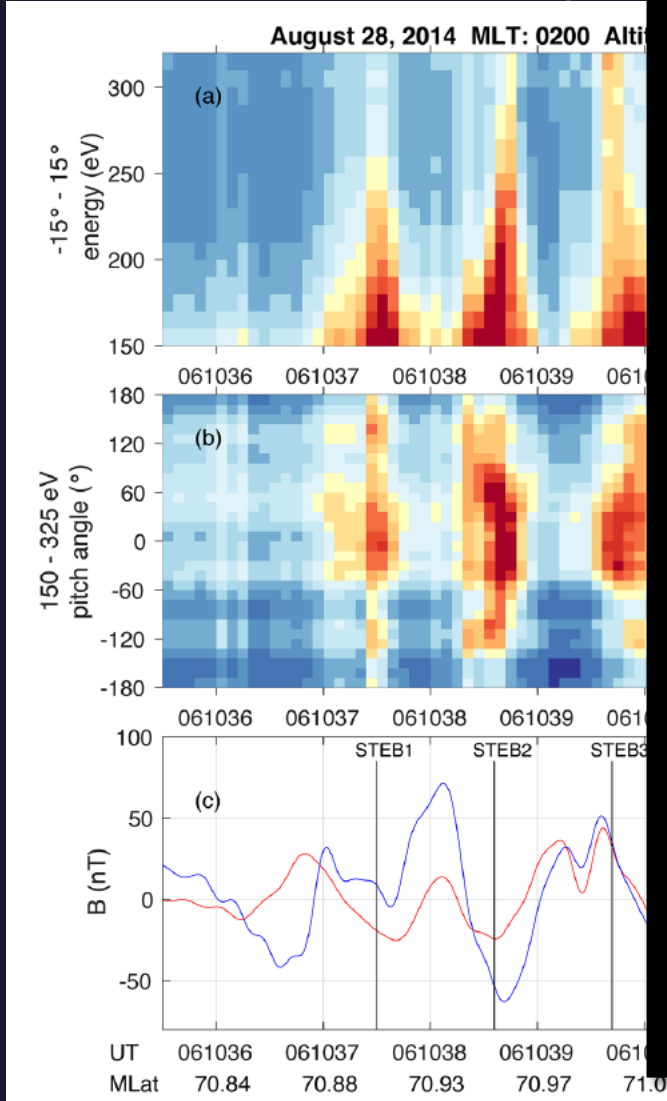
Auroral Dynamics *Alfvén Resonator*



Wu, J., Knudsen, D. J., Shen, Y., & Gillies, D. M. (2021). e-POP observations of Suprathermal electron bursts in the ionospheric Alfvén resonator. *Journal of Geophysical Research: Space Physics*, 126, e2020JA028005. <https://doi.org/10.1029/2020JA028005>

Miles, D. M., Mann, I. R., Pakhotin, I. P., Burchill, J. K., Howarth, A. D., Knudsen, D. J., ... Yau, A. W. (2018). Alfvénic dynamics and fine structuring of discrete auroral arcs: Swarm and e-POP observations. *Geophysical Research Letters*, 45. <https://doi.org/10.1002/2017GL076051>

Auroral Dynamics *Alfvén Resonator*



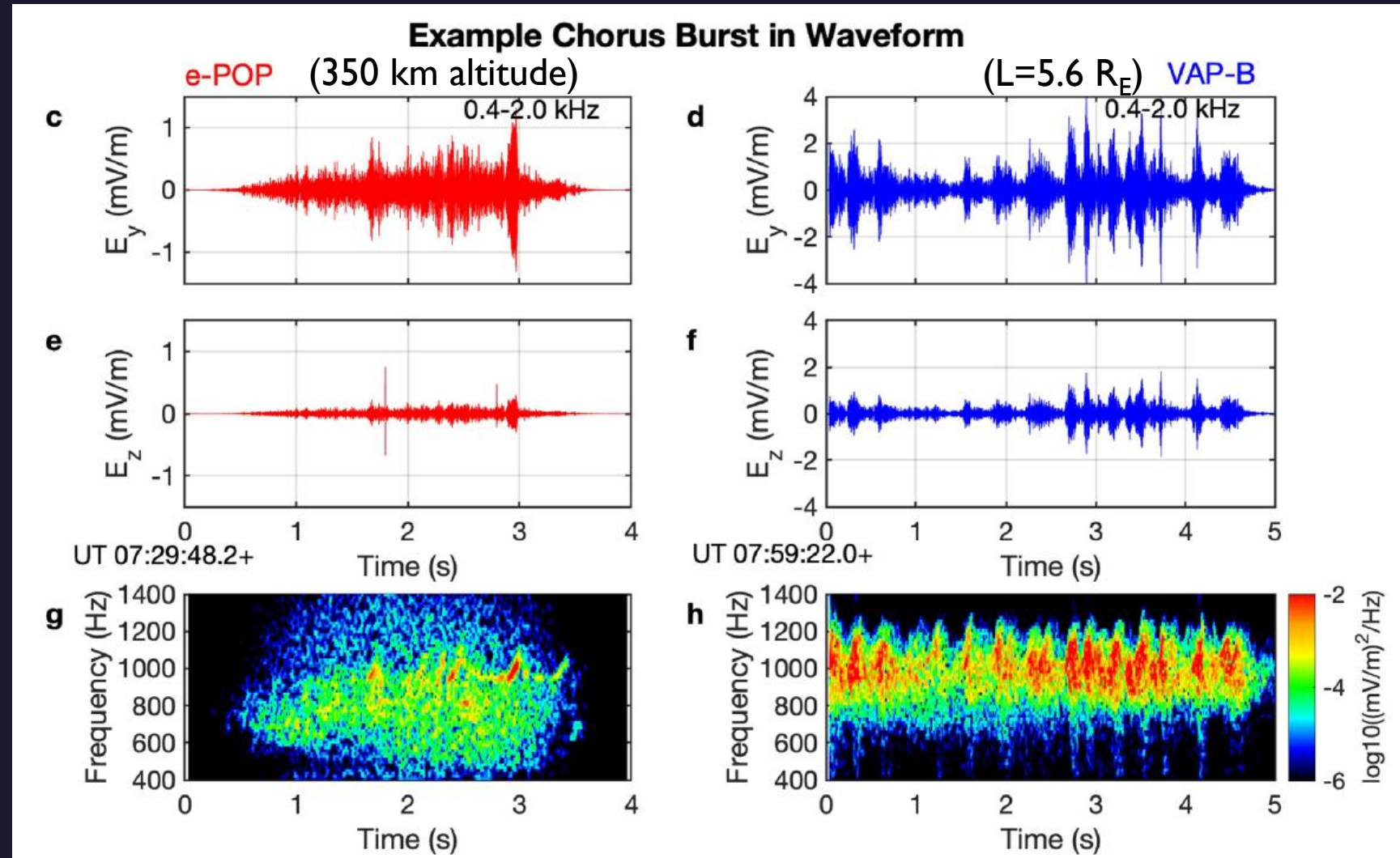
Wu, J., Knudsen, D. J., Shen, Y., & Gillies, D. M. (2021). e-POP observations of Suprathermal electron bursts in the ionospheric Alfvén resonator. *Journal of Geophysical Research: Space Physics*, 126, e2020JA028005. <https://doi.org/10.1029/2020JA028005>

Miles, D. M., Mann, I. R., Pakhotin, I. P., Burchill, J. K., Howarth, A. D., Knudsen, D. J., ... Yau, A. W. (2018). Alfvénic dynamics and fine structuring of discrete auroral arcs: Swarm and e-POP observations. *Geophysical Research Letters*, 45. <https://doi.org/10.1002/2017GL076051>

M-I-T Coupling *Ducted Chorus Waves*



- Chorus wave propagation from the magnetosphere to the ionosphere to the ground
- Waves guided by density crests
- Important for relativistic electron precipitation from the radiation belts



Shen, Y., Chen, L., Zhang, X.-J., Artemyev, A., Angelopoulos, V., Cully, C. M., et al. (2021). Conjugate observation of magnetospheric chorus propagating to the ionosphere by ducting. *Geophysical Research Letters*, 48, e2021GL095933. <https://doi.org/10.1029/2021GL095933>

Data Filtering

<https://edex.phys.ucalgary.ca>



Filter e-POP data by:

- Date/Time
- Geophysical parameters
 - K_p
 - F10.7
 - Etc.
- Spacecraft constraints
 - Position
 - Attitude
 - Instruments on
 - Etc.
- Planned experiments
 - SuperDARN
 - Swarm
 - Conjunctions
 - Etc.

Guest eDEX Web x +
https://edex.phys.ucalgary.ca

eDEX (e-POP Data Explorer) CASSIOPE ESA
Data Handbook API Documentation

Output Product Selection Date Constraints Geophysical Constraints e-POP Constraints Planned Experiment Constraints Query Builder Results

Output Product Selection
Choose which e-POP products will be returned in the results:

CASSIOPE: Attitude Quaternions and YPR Bus Telemetry Legacy Ephemeris and Attitude Orbit Ephemeris SP3

e-POP: Quicklook Instrument Data Availability

CER: Quicklook TEC Ground Receiver Data

FAI: Quicklook Summary PNG Images Lv1 HDF5 Images

GAP: Quicklook Lv1 LOS TEC VTEC RINEX Observation

IRM: Quicklook Summary Surface Sensor Current Lv0b

MGF: Quicklook Summary Residual 1 sps Lv1b CDF 160 sps Lv1b CDF

NMS: Lv0b Quicklook Quicklook Velocity Quicklook Position

RRI: Quicklook Lv1 HDF5

SEI: Quicklook Summary Lv0b

Next Step...

Selections

Selected Output Products
<No Output Products Selected>

Constraints
<No Constraints Selected>

Query

Data Filtering



Example: RRI quicklook plots when $K_p > 5$, southern hemisphere, altitude > 500 km

The screenshot shows the eDEX (e-POP Data Explorer) interface. At the top, there are logos for eDEX, CASSIOPE, and ESA, along with buttons for 'Data Handbook' and 'API Documentation'. Below the logos are navigation tabs: 'Output Product Selection', 'Date Constraints', 'Geophysical Constraints', 'e-POP Constraints', 'Planned Experiment Constraints', 'Query Builder', and 'Results' (which is highlighted).

The 'Results' section displays a query: `(rri.Quicklook) WHEN ('Geophysical Parameters':'Kp*10' :: > ('50'), 'Spacecraft Position':'Geographic Latitude (deg)' :: < ('0'), 'Spacecraft Position':'Altitude (km)' :: > ('500')) USING QUERY (1 AND 2 AND 3)`. It lists 17 files, each with a checkbox, filename, and size. A 'Fetch Results...' button is visible below the list, along with a 'Delivery Email Address' field and a 'Download Results...' button. The 'Fetch Results...' button is highlighted in blue.

The 'Selections' section on the right shows 'Selected Output Products' with a button for 'rri.Quicklook'. Below that is a 'Constraints' table:

ID	Field	Operator	Value
1	'Geophysical Parameters':'Kp*10'	'>'	50
2	'Spacecraft Position':'Geographic Latitude (deg)'	'<'	0
3	'Spacecraft Position':'Altitude (km)'	'>'	500

Below the constraints table is a 'Query' section showing the query: `1 AND 2 AND 3`.

At the bottom right, the URL <https://edex.phys.ucalgary.ca> is displayed in yellow text.

Data Filtering



Example: RRI quicklook plots when $K_p > 5$, southern hemisphere, altitude > 500 km

The screenshot shows the eDEX (e-POP Data Explorer) interface. At the top, there are logos for eDEX, CASSIOPE, and ESA, along with buttons for 'Data Handbook' and 'API Documentation'. Below the logos are navigation tabs: 'Output Product Selection', 'Date Constraints', 'Geophysical Constraints', 'e-POP Constraints', 'Planned Experiment Constraints', 'Query Builder', and 'Results' (which is highlighted in blue).

The 'Results' section displays a query: `(rri.Quicklook) WHEN ('Geophysical Parameters':'Kp*10' :: > ('50'), 'Spacecraft Position':'Geographic Latitude (deg)' :: < ('0'), 'Spacecraft Position':'Altitude (km)' :: > ('500')) USING QUERY (1 AND 2 AND 3)`. It shows 17 files, each with a checked checkbox, a filename, and a size. A 'Fetch Results...' button is visible, along with a 'Delivery Email Address' field and a 'Download Results...' button. The fetched data volume is 26.61MB.

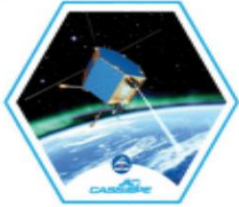
The 'Selections' section on the right shows 'Selected Output Products' with 'rri.Quicklook' selected. Below this is a 'Constraints' table, which is highlighted with a red box. The table has columns for ID, Field, Operator, and Value.

ID	Field	Operator	Value
1	'Geophysical Parameters':'Kp*10'	'>'	50
2	'Spacecraft Position':'Geographic Latitude (deg)'	'<'	0
3	'Spacecraft Position':'Altitude (km)'	'>'	500

Below the constraints table is a 'Query' section showing '1 AND 2 AND 3'. At the bottom right of the interface, the URL <https://edex.phys.ucalgary.ca> is displayed in yellow text.

e-POP Data

Custom Quicklook



e-POP Payload Quicklook



Output Plot Selection

Choose which plots to display in your quicklook:

Order of selection will display top to bottom*

EPHEMERIS: Latitude Longitude Altitude Magnetic Latitude Magnetic Local Time Eclipse Attitude

TELEMETRY: ADCS Mode Torque Rods MGF Temperature Wheel Temperature Wheel Speed

IRM: Hit Detection Surface Sensor Current Average

FAI: Camera - Near Infrared Camera - Visible

MGF: Outboard Sensor NEC CHAOS DELTA Outboard Sensor CRF Inboard Sensor CRF Sensor Deltas

CHAOS

RRI: Sonogram A Sonogram B

*eclipse always displayed at the bottom

Date Range (UTC)

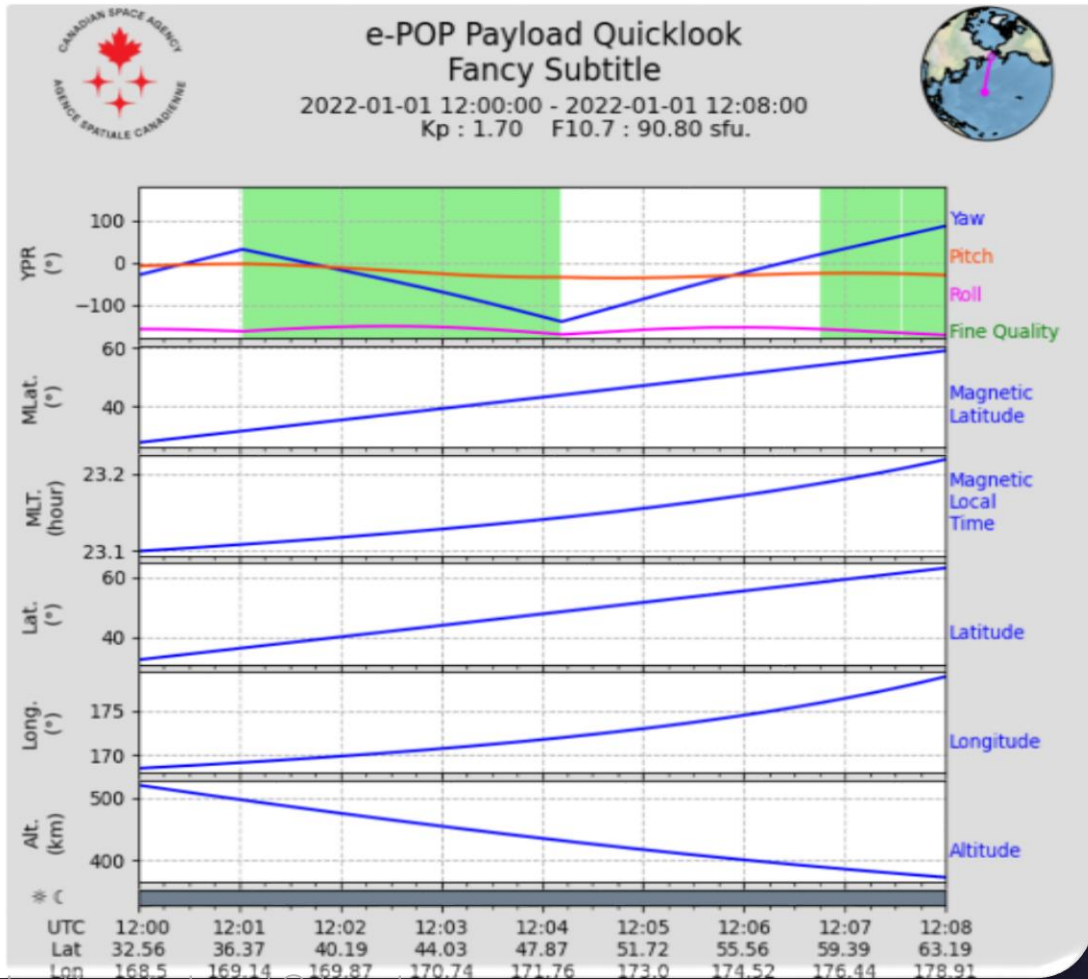
A time range of 10 minutes is typical.

Start Date 2022-01-01 12:00:00

End Date 2022-01-01 12:08:00

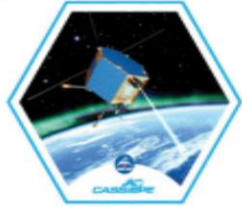
Subtitle

Fancy Subtitle



e-POP Data

Custom Quicklook



UNIVERSITY OF CALGARY

e-POP Payload Quicklook



Output Plot Selection

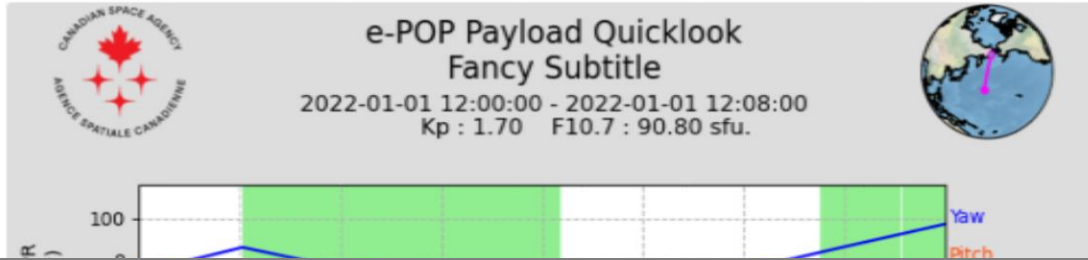
Choose which plots to display in your quicklook:

Order of selection will display top to bottom*

EPHEMERIS: Latitude Longitude Altitude Magnetic Latitude Magnetic Local Time Eclipse Attitude

TELEMETRY: ADCS Mode Torque Rods MGF Temperature Wheel Temperature Wheel Speed

IRM: MGF Radiation Solar Constant



<https://payloadquicklook.phys.ucalgary.ca>

RRI: Sonogram A Sonogram B

*eclipse always displayed at the bottom

Date Range (UTC)

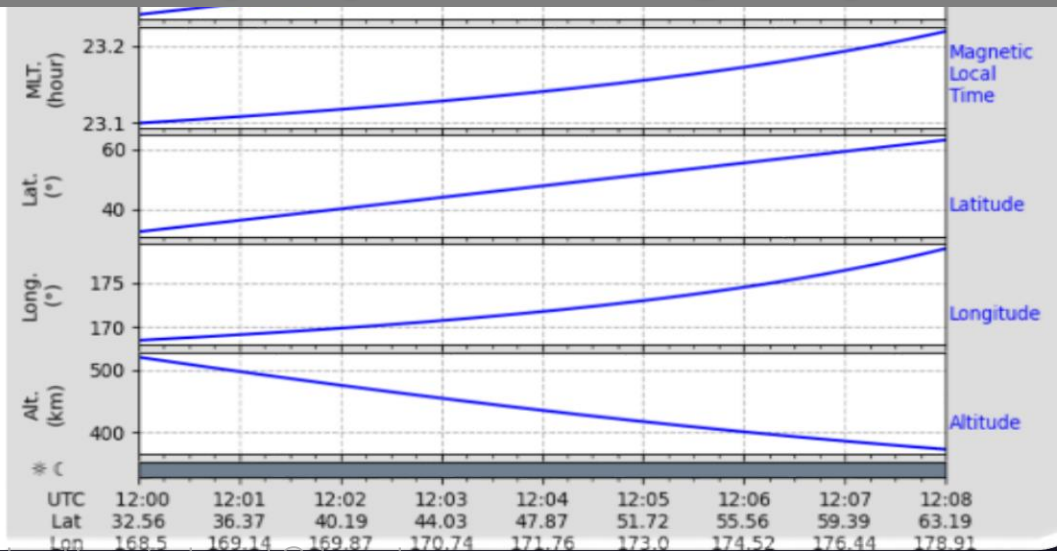
A time range of 10 minutes is typical.

Start Date 2022-01-01 12:00:00

End Date 2022-01-01 12:08:00

Subtitle

Fancy Subtitle





Direct data download

<https://epop-data.phys.ucalgary.ca>

Filtering with multiple data sets

<https://edex.phys.ucalgary.ca>

More about CASSIOPE/e-POP/Swarm-E

<https://epop.phys.ucalgary.ca>



Canadian Space Agency

Agence spatiale canadienne



Canada

MDA



Thank You!

Andrew Howarth

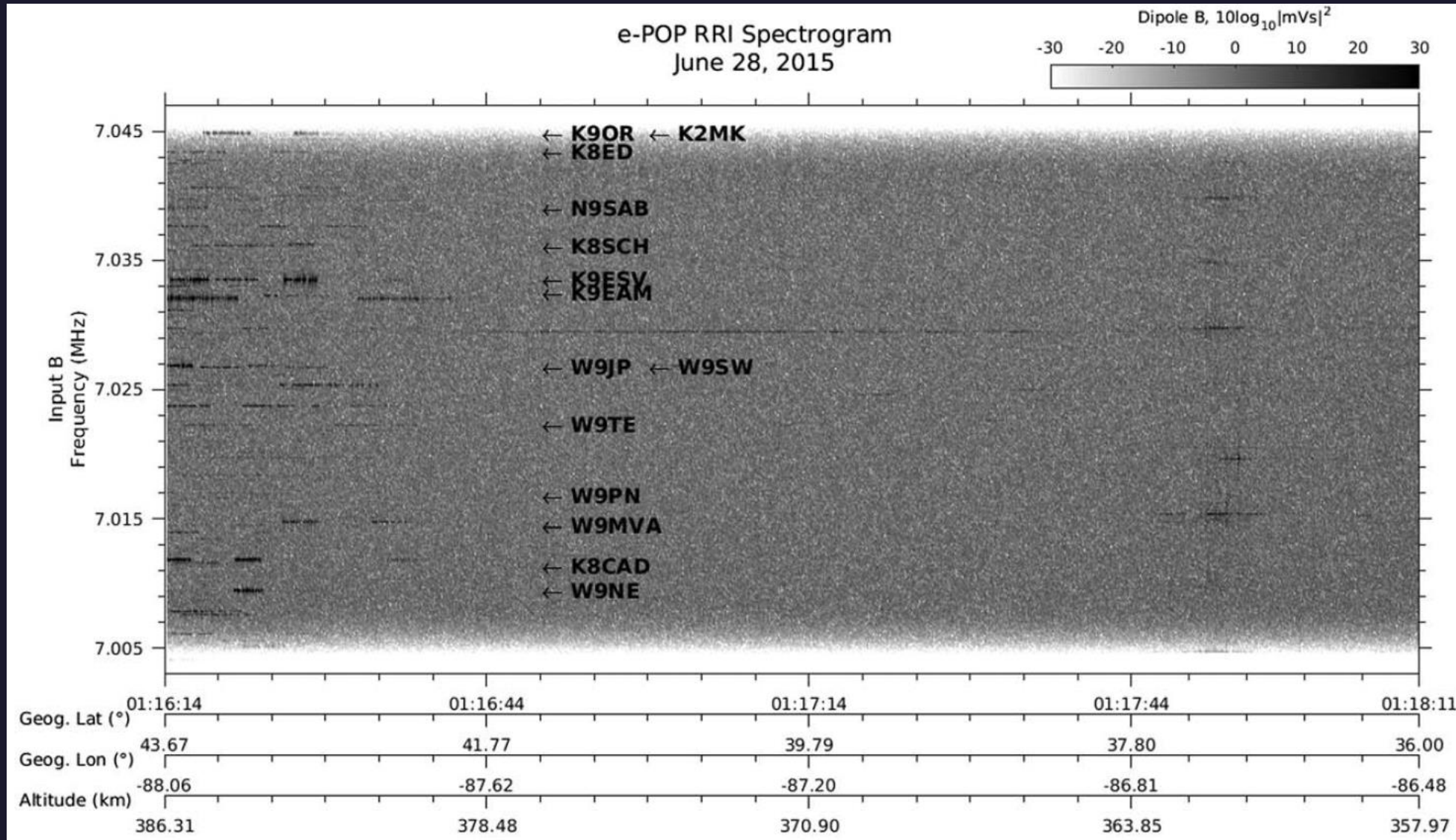
howarth@phys.ucalgary.ca

<http://epop.phys.ucalgary.ca>



Radio Science

Citizen Science



Perry, G. W., Frissell, N. A., Miller, E. S., Moses, M., Shovkoplyas, A., Howarth, A. D., & Yau, A. W. (2018). Citizen radio science: An analysis of amateur radio transmissions with e-POP RRI. *Radio Science*, 53, 933–947.
<https://doi.org/10.1029/2017RS006496>